Giant tsunami monitoring, early warning and hazard assessment

Nobuhito Mori[1 †], Kenji Satake[2], Daniel Cox[3], Katsuichiro Goda[4], Patricio A. Catalan[5], Tung-Cheng Ho[6], Fumihiko Imamura[7], Tori Tomiczek[8], Patrick Lynett[9], Takuya Miyashita[10], Abdul Muhari[11], Vasily Titov[12], and Rick Wilson[13]

[1] Disaster Prevention Research Institute, Kyoto University, Kyoto, Japan; ORCID ID: 0000-0001-9082-3235

[2] Earthquake Research Institute, University of Tokyo, Tokyo, Japan; ORCID ID: 0000-0002-3368-3085

[3] School of Civil and Construction Engineering, Oregon State University, Corvallis, OR, United States; ORCID ID: 0000-0002-8270-361X

[4] Department of Earth Sciences, Western University, London, Canada; ORCID ID: 0000-0003-3900-2153

[5] Departamento de Obras Civiles, Universidad Técnica Federico Santa María, Valparaíso, Chile; ORCID ID: 0000-0002-6567-5776

[6] Disaster Prevention Research Institute, Kyoto University, Kyoto, Japan; ORCID ID: 0000-0002-3678-8288

[7] International Research Institute of Disaster Science, Tohoku University, Sendai, Japan; ORCID ID: 0000-0001-7628-575X

[8] Department of Naval Architecture and Ocean Engineering, United States Naval Academy, Annapolis, MD, United States; ORCID ID: 0000-0003-4116-7547

[9] Department of Civil and Environmental Engineering, University of Southern California, Los Angeles, United States; ORCID ID: 0000-0002-2856-9405

[10] Disaster Prevention Research Institute, Kyoto University, Kyoto, Japan; ORCID ID: 0000-0002-3196-2726

[11] Badan Nasional Penanggulangan Bencana, Jakarta, Indonesia; ORCID ID: 0000-0002-4522-8258

[12] Pacific Marine Environmental Laboratory, National Oceanic and Atmospheric Administration, Seattle, WA, United States; ORCID ID: 0000-0002-1630-3829

[13] California Geological Survey, Californian Department of Conservation, Sacramento, CA, United States; ORCID ID: 0000-0003-3629-2167

† email: mori@oceanwave.jp

[H1] Abstract

Earthquake-triggered giant tsunamis can cause catastrophic disasters to coastal populations, ecosystems and infrastructure over 1000s km. In particular, the scale and tragedy of the 2004 Indian Ocean (about 230,000 fatalities) and 2011 Japan (22,000 fatalities) tsunamis prompted global action to mitigate the impacts of future disasters. In this Review, we summarize the progress in understanding tsunami generation, propagation, and monitoring, with a particular focus on developments in rapid early warning and long-term hazard assessment. Dense arrays of ocean-bottom pressure gauges in offshore regions provide real-time data of incoming tsunami wave heights, which combined with advances in numerical and analogue modelling, have enabled the development of rapid tsunami forecasts for near-shore regions (within 3 minutes of an earthquake in Japan case). Such early warning is essential to give local communities time to evacuate and save lives. However, long-term assessments and mitigation of tsunami risk from probabilistic tsunami hazard analysis (PTHA) are needed so that comprehensive disaster prevention planning and structural tsunami countermeasures can be implemented by governments, authorities, and local populations. Future work should focus on improving tsunami inundation, damage risk and evacuation modeling and reducing the uncertainties of PTHA associated with the unpredictable nature of megathrust earthquake occurrence and rupture characteristics.

Website Summary:

The scale and tragedy of the giant tsunamis in 2004, 2010 and 2011 led to a revolution in tsunami monitoring. This Review assesses the advances in tsunami observation, monitoring and hazard assessment, which have allowed near-real time early warning systems to be developed.

[H1] Key Points

- The scale and tragedy of the 2004 Indian Ocean Tsunami and the 2011 Tohoku Tsunami prompted the widespread deployment of tsunami observation networks and the development of tsunami modelling, which have enabled tsunami early warning systems to approach near real-time inundation forecasts based on the dense arrays of offshore observation data.
- Earthquake magnitude alone does not characterize the size or impact of the ensuing tsunami disaster. The tsunami source (such as earthquake location and rupture characteristics), coastal geomorphic features and exposure of densely populated areas play key roles in tsunami behaviour, inundation extents and the level of impact.
- Reproducing the inundation depth and flow velocity of tsunamis that run up to urban areas is important for future tsunami risk mitigation. Combination of numerical and physical models are needed to better understand the complex interactions between building layouts, structures, debris and non-hydrostatic flow.
- Long-term assessments of the tsunami will give a condition for soft and hardware countermeasures. Hardware or structure measures (such as sea walls) can reduce life, and asset and software or non-structural measures (such as evaluation, assessments, and planning) can reduce life losses.

- The probabilistic tsunami risk assessment (PTHA) is a recent option to consider the variability of tsunami conditions for risk mitigation. The PTHA can be used for engineering design, and tsunami inundation maps at different return period levels, which can be used for development of local and regional hazard mitigation plans

[H1] Introduction

Giant tsunamis are generated by shallow subduction zone [G] earthquakes (Mw ≥ 8.5) that rupture the seafloor, displacing the ocean and generating peak wave heights over 10-20 m high, roughly. These giant tsunamis cause catastrophic disasters as they rapidly inundate coastal areas within a few minutes after the arrival and giving little time or information (or both) for authorities to provide warning due to location of large slips along the subduction zone. For example, the number of causalities of the 2011 Tohoku Earthquake Tsunami exceeded 22,000, even though Japan is relatively well-prepared for earthquakes and tsunamis. The tragedy of the 2004 Indian Ocean Tsunami was even greater, as over 230,000 people lost their lives across 14 countries, it is thought to be the deadliest tsunami in history. Both the 2004 and 2011 tsunamis were much larger than predicted by authorities at the time, and as a result, the warnings given underrepresented the scale of these events. To mitigate the effects of future extreme tsunami disasters, an integrated approach that combines fundamental research on tsunami generation, propagation, and inundation with real-time warning (forecasts) and long-term assessment [G] of tsunami hazard and risk assessments [G] is necessary (Fig. 1).

The primary cause of giant earthquake-triggered tsunamis is rapid seismic displacement of the megathrust fault [G] at subduction zones[1] (Fig.1, 2), hence they are sometimes termed megathrust earthquake-tsunamis [G]. Earthquakes that can rupture the seafloor are typically ≥8.5 Mw earthquakes, <15 km deep and that generate a large amount of fault slip (over 10 m) over a large area (over a few hundred km) in a shallow area along the trench axis. For example, the earthquake magnitude was 9.1, the size of fault was 500 km by 200 km at the depth of 5 – 20 km, and 30 m or larger slip was occurred in the 2011 Tohoku Earthquake.

Research on megathrust earthquakes and tsunamis has surged globally since the 2004 Indian Ocean Tsunami and accelerated further after the 2010 Maule Tsunami in Chile and the 2011 Tohoku Tsunami in Japan. The tragedy of these giant tsunamis prompted action to deploy more extensive geophysical instrumentation networks, which are providing better resolution seismic and tsunami monitoring that is essential for delivering rapid early warning to local communities and for increasing the understanding of megathrust earthquake tectonics. Advances in increased measurement networks, model development, computational power, and joint seismic-tsunami risk methodology have also progressed tsunami-related science and engineering technology development since these events.

The understanding and development of tsunami observation networks have dramatically improved. For example, after the 2004 Indian Ocean Tsunami, the global tsunami observation network was expanded to 60 systems of DART [G] (Deep-ocean Assessment and Reporting of Tsunamis) network across the Pacific, Atlantic and Indian oceans nowadays. As such, the observation network for far-field tsunamis was substantially improved over the Pacific Ocean. Likewise, after the 2011 Tohoku Tsunami, denser observation networks, Seafloor observation network for earthquakes and tsunamis along the Japan Trench (S-net [G]) and Deep Ocean-floor Network system for Earthquakes and Tsunamis (DONET/DONET2 [G]), were established along the Pacific Japanese coast. These network was expanded to 200 from 3 tsunami sensors since 2013 and can reduce the time of early-warning release and can increase the accuracy of tsunami height.

Such dense monitoring networks have provided enough data to support the development of tsunami early warning (TEW) [G] systems for near-field tsunamis[G] in both Japan, the United States, and several other countries. These approaches integrate near-real time seismic and tsunami observations, which have been enabled by increases in computing power. TEW gives the time to evacuate and is critical for near-field tsunamis because it's short arrival time (<10-30 mins for some locations). These advances have contributed to the establishment and wider acceptance of probabilistic tsunami hazard assessments[G]. In addition, long-term assessments of tsunami hazards (next a few decades or longer) provide essential information for social scientists, economists, urban planners, and engineers to implement disaster risk reduction plans and policies, such as structural and non-structural mitigation and evacuation planning.

In this Review, we summarize the progress in understanding historical tsunamis, the development of the latest observation networks and TEW systems. Furthermore, we summarize megathrust subduction zone modeling for tsunamis, model development of tsunami propagation and inundation process, and long-term assessment with applications to hazard assessment and risk mitigation.

[H1] Historical Giant Tsunamis

Multiple giant tsunami events have occurred in the last ~20 years, which caused devastating impacts and raised global awareness of tsunami disasters. This section briefly summarizes four of these major tsunamis since the turn of the millennium (Fig. 2), the instrumental records of which have provided unprecedented insight into tsunami generation and propagation and highlighted flaws in the early warning systems of the time. In particular, the impact of the 2004 and 2011 events were a much larger magnitude than local communities anticipated before the tsunamis hit coastal regions. These experiences accelerated technology developments into early warning systems and prompted increased actions to educate residence in tsunami awareness and preparedness.

[H2] 1960 and 2010 Chilean Tsunami

The eastern Pacific seaboard is one of the most seismically active zones in the world due to the subduction of the Nazca Plate under the South American Plate, with convergence rates that reach up to 70 mm per year [2]. As a result, the region produced five megathrust (M_W >= 8.0) earthquakes since 1922[3]. For example, paleotsunami [G] evidence[4,5] from Chile has been used to estimate a recurrence interval of 285 years for earthquakes larger than Mw9.0 in this region[6].

The largest instrumentally recorded earthquake was the May 22, 1960, Mw9.5 Valdivia event, which ruptured more than 1,000 km of seafloor from 37°S to 45°S[7-9]. The 1960 earthquake cause 18 m high tsunami along the Chilean coast and triggered a trans-Pacific tsunami that was less documented in the near-field (along the South American west coast) because it affected sparsely populated areas. However, the tsunami was recorded by far-field wave recording stations throughout the Pacific Ocean[9,10]. It caused damage and destruction across the Pacific[11], including in Hawaii, where 61 people died owing to waves up to 10.7 m, and Japan, where waves reached up to 6.3 m causing 138 fatalities[11].

Chile did not experience a megathrust tsunami again until 50 years later, when the segment immediately north of the 1960 event ruptured on February 27, 2010 in a Mw8.8 earthquake off the coast of the Maule Region (35°26'S, 71°40'W). The 2010 earthquake fault size was 700 km long at depth of 35 km with slip of almost 10 meters It caused 3 m tsunami along the Chilean coast and expanded over the Pacific Ocean. The 2010 tsunami caused major damage and 124 fatalities in the coastal regions (Valparaiso, Santiago and Maule) and islands of Chile[12], affecting a more densely populated area than previous tsunamis in the 500 years prior[13]. It was the first time to check the usefulness of DART system over the Pacific after the 2004 Indian Ocean Tsunami.

The most striking feature of the 2010 event was that run-up height distributions showed a large variability over a 1,000 km stretch of the Chilean coast, with an average run-up height of 7 m and reaching up to 29 m in some extreme locations[12], which can be explained by the edge waves [G] along the continental shelf amplified the tsunami waves[13]. Based on the model tests have shown that the slip distribution affects edge waves and the combination of direct tsunami waves from the source and substantial edge waves along the coast significantly amplified total tsunami heights along the coast[13].

These two events provided many lessons[14]. From a physical standpoint, they highlighted that earthquake magnitude alone is insufficient to characterize the impact of a tsunami disaster, although two events were quite large in magnitudes. The details of the source, coastal geomorphic features, and exposure play key roles in tsunami behavior and the related disaster[15].

[H2] 2004 Indian Ocean Tsunami

The 2004 Indian Ocean Tsunami was caused by the Sumatra-Andaman earthquake, which occurred on a low-angle trust fault at the subduction zone between the Indian and Sunda Plates[16]. The magnitude [G] of this earthquake was initially measured magnitude 8.5 in the first hour and moment magnitude [G] Mw9. 0 by Global CMT solution 19 hours after the earthquake[17], while the estimated moment magnitude [G] was, about 2.5 times larger, up to Mw9.3[18,19]. The epicenter was located off the west coast of northern Sumatra Island at a depth of 30 km[19], with the rupture extending out northwards by more than 1,200 km over a period of ~8 minutes[20,21]. This extensive fault rupture generated a massive tsunami with run up heights up to 51 m[23, 24] and maximum inundation distances up to 939 m[25]. The scale of this event resulted in severe losses and fatalities along the coastline areas of the Indian Ocean[7]. The earthquake and subsequent tsunami caused over ~230,000 fatalities[13] across 10 countries in South Asia and East Africa, and is thought to be the deadliest tsunami in history.

The tsunami propagated eastward towards Indonesia, Thailand, Myanmar, Malaysia, and the nearby islands within a few hours. Indonesia was first to be impacted, with the tsunami waves arriving within 30 minutes after the earthquake[26]. Thailand was impacted next, where tsunami waves with run-up heights larger than 10 m (and even up to 19.6 m, ref.[25]) hit the coast about two hours after the earthquake[25]. The tsunami also propagated westward to Sri Lanka, where the south coast was impacted by intensive tsunami waves[24] with inundation distances of up to 390 m and runup heights of up to 12.5 m[27]. The Indian mainland and islands were also impacted by the tsunami about two hours after the earthquake. The east coast of India was most damaged, where the maximum runup of 5 m and inundation distance of 2 km were reported in Nagapattinam, Tamil Nadu state and Pondicherry (Puducherry) city[24,28]. The tsunami propagated ~5,000 km across the Indian Ocean to Somalia and the East African coast in about 7.5-8 hours[29], where it caused large run-up heights up to 9-m high [29] and inundation distances of a few hundred meters[29]. There was not TEW system in Indian Ocean at that time. No tsunami warning issue was released these countries, although there was enough time to evacuate for the most of counties. DART system installed in Indian Ocean as well as increasing number of systems in other oceans after this event.

The tsunami was also detected in the Atlantic and Pacific Oceans[30] by numerous tide gauges, wave gauges, and ocean bottom pressure (OBP) gauges, such as DART stations[31]. In addition to ground observatories, the 2004 tsunami was the first tsunami for which the wavefields were captured by satellite altimeters[32, 33]. With these observations, analyses have been performed with in-situ and satellite data[34-36]. The satellite altimeter data could measure spatial distribution of tsunami waveform over a few hundred kilometers. The combined two different observation data could improve the initial source estimation more accurately[34]

The 2004 tsunami immediately aroused an intense global concern about tsunami hazards. Since this event, tsunami monitoring and warning systems have been successfully developed in many countries that are at risk of tsunami hazards. For example, the German Indonesian Tsunami Early Warning System (GITEWS) Project for Indonesia was established and leaded to the first TEW alert in Indonesia[37].

[H2] 2011 Tohoku Tsunami

The 2011 Tohoku Tsunami was generated along the northern Pacific coast of Japan due to the Mw9.1 earthquake on March 11, 2011[Error! Reference source not found.-39] . The magnitude was underestimated by 7.9 in the first 20-30 minutes, which was critical for timely tsunami evacuation in coastal areas near the source[40]. This earthquake and the induced tsunami caused fatalities of 19,729 and destroyed 121,996 houses[39].

The earthquake epicenter was located off the coast of Miyagi prefecture in the Tohoku region, Japan[41]. The fault rupture of the earthquake lasted for more than 3 minutes, and the seismic waves initially propagated strongly toward Fukushima, Miyagi, and Iwate prefectures. Later, strong tremors spread toward Aomori in the north and Chiba in the south. The estimated main fault slip area was delineated with active aftershocks that occurred over 500 km wide area off the Tohoku coast with a fault slip of more than 30 m (up to 60 m possible slip was estimated [42]). The resulting seafloor uplift caused more than 6 m changes in sea level[43], resulting in a giant tsunami.

There were two notable characteristics of this event. One was the scale of the maximum runup height of over 40 m on the Sanriku ria coast and the inundation extent over 1-3 km, which was similar to the past 1611 Keicho, 1896 Meiji, and 1933 Showa Sanriku Tsunamis[44]. The destructive power the incoming and receding waves was enormous. Many villages and towns were totally washed out including houses, city halls and others.

The other notable characteristic was related to the tsunami in the low-lying southern Sendai Plain, with a maximum nearshore tsunami height of 15 m. The scale of the tsunami in this area far exceeded the anticipated scenario of the Miyagi-oki tsunami evaluated before 2011 - indeed, the inundation range was 10 times larger than predicted (up to 5 km from the coastline) by Earthquake Research Committee of the Headquarters for Earthquake Research Promotion under MEXT[45], and the prolonged inundation was experienced over a wide area, hampering the rescue and restoration activities.

The tsunami propagated from deep to shallow waters and reached the coastal area within 20-30 minutes of the earthquake occurrence[44]. Tsunami wave amplification was observed along the Sanriku ria coast. Furthermore, coastal areas of the southern Tohoku region experienced the most substantial damage ever recorded. In particular, the tsunami generation area extended to areas offshore of Miyagi and Fukushima prefectures. A huge tsunami hit the coast of Sendai and Fukushima directly. Compared to Sanriku, these areas were less well prepared and consequently suffered greater property and human losses. The importance of tsunami scenarios and related preparation was confirmed by these comparisons.

A total of more than 5,000 tsunami trace observations were surveyed by July 2011, resulting in an extremely large and spatially dense dataset of tsunami trace height[44,46] (note: tsunami trace height means the elevation with respect to sea level of tsunami traces, such as debris or flow markers in structures which corresponds to runup or inundation height). For example, in the Sanriku region, areas with trace heights of 20 m or more extend over 290 km from north to south, and locations with trace heights of 30 m or more exist near Miyako City and Onagawa Town. Therefore, the runup height was notably larger than the nearshore tsunami height in these areas, indicating the affect of local amplification during the inland runup process.

The 2011 Tohoku Earthquake resulted in strong ground motion with tsunami inundation and flooding, destruction of coastal structures, damage to coastal forests, houses, buildings, and infrastructure, erosion and sedimentation, and changes in topography due to destruction and movement. In addition, the tsunami generated debris, offshore tsunami, drifting of ships, spills, and fires of combustible materials, and it caused damage to transportation networks such as roads and railroads, ports and airports, and critical facilities, such as nuclear and thermal power plants. In this way, great human damage over 22,000 causalities, economic damage and infrastructure damage (direct damage 9.6 trillion yen), were caused. Although they were reduced by the disaster prevention and reduction preparations that were being implemented at that time (for example, strengthening infrastructure development, disaster prevention education, evacuation system, and cooperation agreement for restoration), the damage was very extensive and thousands of lives were lost[47,48]. Therefore, disaster mitigation should be evaluated quantitatively to help preparations for future events.

[H1] Observation Systems and Early Warning

Currently, there are many tsunamis observation and tsunami early warning systems (TEWS) in the world. Here, we focus on the global DART observation network and two particular TEWS in the United States and Japan as examples to demonstrate the history and scope of these systems.

[H2] DART system

DART system is the real-time tsunami monitoring systems, developed by Pacific Marine Environmental Laboratory (PMEL), National Oceanic and Atmospheric Administration (NOAA). DART system consists of a pressure sensor at seafloor bottom to detect tsunamis and moored surface buoy for real-time communications via satellites. DART system can measure tsunami waveform at 15-minute intervals in regular modes and becomes every 15 seconds in event mode.

First DART buoy was tested in 2000 and DART system with 6 tsunami sensors deployed near regions U.S coast after that. The global tsunami observation network by DART was expanded to 60 systems across the Pacific, Atlantic and Indian oceans. It has been used for TEW system over the world now.

[H2] United States network

The first Tsunami Warning Center in the U.S. was established following the 1946 Aleutian Islands Earthquake and Tsunami (Mw8.6) and uses networks of seismic and sea-level observation systems to detect and forecast tsunamis. These networks are owned and operated by a number of domestic and international organizations, including the National Oceanic and Atmospheric Administration (NOAA). The collected data are combined with numerical models to continuously refine their messages with more accurate, targeted, and detailed information.

NOAA operates two 24-hour tsunami centers. The Pacific Tsunami Warning Center (PTWC) in Honolulu, Hawaii, directly serves the Hawaiian Islands, the U.S. Pacific and Caribbean territories, and the British Virgin Islands and is the primary international forecast center for the Pacific and Caribbean. In addition, as a result of the 1964 Mw9.2 Great Alaska earthquake, which killed over 100 people in Alaska, Oregon, and California, the National Tsunami Warning Center (NTWC) was established in Palmer, Alaska, and serves Alaska, Canada, and the continental U.S. For tsunami forecasts, the PTWC utilizes the Real-time Forecast of Tsunamis (RIFT) model[49], which utilizes the passing tsunami waves to forecast the maximum deep-ocean tsunami height as well as the coastal maximum tsunami wave height. The NTWC uses the numerical model ATFM (Alaska Tsunami Forecast model)[50] to forecast the propagation and inundation of tsunamis in the Pacific and Atlantic Oceans. ATFM pre-computes hundreds of hypothetical cases, which are accessed and calibrated with observations during a real event to have an immediate forecast. In addition, both Tsunami Warning Centers use the Short-term Inundation Forecasting for Tsunamis (SIFT) model developed by the NOAA Pacific Marine Environmental Laboratory[51] (PMEL) to forecast tsunami arrival times, heights, and inundation based on observations in the deep ocean.

NOAA relies on in-water instruments and observation systems for tsunami monitoring and forecasting. NOAA's National Data Buoy Center operates and maintains the U.S. network of DART systems, which were developed by NOAA's PMEL for the early detection, measurement, and real-time reporting of tsunamis in the open ocean. Closer to shore, networks of coastal water-level stations are used to confirm tsunami arrival times and nearshore tsunami heights as well as determine when to downgrade or cancel a tsunami Advisory or Warning. In the U.S., most of these stations are operated and maintained by NOAA's Center for Operational Oceanographic Products and Services and the Tsunami Warning Centers. NOAA is also exploring integrating other observation systems into their tsunami detection system, including the Global Navigation Satellite System (GNSS) and ocean-bottom cable systems.

Tsunami warning messaging is relayed from the Tsunami Warning Centers to regional NOAA National Weather Service offices, state-level Operation Centers, local emergency managers, and the public. There are four levels of tsunami alerts in the U.S.: Information Statement, Watch, Advisory, and Warning. The Advisory level is used when nearshore tsunami heights are between 0.3 m and 1 m for a section of coastline and require responses by harbors and beach officials. The Warning level is called for areas under threat from tsunami heights greater than 1 m, which would require evacuation on land. Tsunami alert messaging is shared through multiple announcement methods for keep redundancy, including NOAA Weather Radio, wireless emergency alerts, radio and television, outdoor sirens, text message alerts, and reverse-call phone messages. For the western coast of the U.S, which is an active tectonic region that includes the Cascadia subduction zone, tsunami messaging is being integrated into earthquake early warning (EEW) platforms and the ShakeAlert® system [G]. The system issued alerts 5 to 10 s for several recent earthquakes.

[H2] Japanese network

Since the 1990's, substantial progress has been made in earthquake and tsunami observation networks in Japan, especially early warning systems. For example, after the 1995 Kobe earthquake (Mw6.9), the Japanese Government deployed nationwide dense networks of high-sensitivity seismographs (Hi-net), broad-band seismographs (F-net), and strong-motion seismographs (K-NET and KiK-net). These seismological observation systems, now unified as MOWLAS[52], have provided basic observational data for the seismic activity of the Japanese Islands. Japan Meteorological Agency (JMA) monitors the seismic activity 24 hours a day, 7 days a week; once an earthquake occurs, JMA reports the recorded seismic intensities in about 2 minutes, and estimated location (latitude, longitude, and depth) and size (magnitude) of the earthquake, as well as the possibility of a tsunami in 3-5 minutes[53]. When the seismic intensity of 5 or larger on the JMA scale is anticipated, which is almost equivalent to Mw≥5, EEW information is issued. The typical lead time between the announcement and the start of large ground shaking is from several to several tens of seconds, providing useful information through TV, radio, or cell phones.

The GNSS has been used to monitor crustal movement by nationwide observation stations (GEONET) and sea levels by offshore buoys[54]. Currently, 18 GNSS buoys, as a part of the Nationwide Ocean Wave Information Network for Ports and Harbours (NOWPHAS) system, are moored at 10 to 20 km distance from shorelines at water depths of 100 to 400 m. The GNSS buoy of the NOWPHAS uses a real-time kinematic

(RTK) algorithm, which utilizes a rover GNSS on a buoy to monitor the sea level and a reference GNSS on a fixed base station on land to reduce the position error of the rover. It provides an accuracy of 4 cm at a distance of 20 km from the base station. Such accuracy is sufficient for tsunami detection, as demonstrated during several events, such as the 2010 Chilean Tsunami[54] and the 2011 Tohoku Tsunami[55].

OBP gauges, which monitor ocean bottom pressure and convert to sea-level heights, detect tsunamis in the deep ocean. Around Japan, more than 200 OBP gauges are connected by seafloor cables (Fig. 3), and the high-resolution high-sampling data are sent to JMA in real-time[56]. The two largest networks are S-net and DONET/DONET2. In the DONET/DONET2 systems, ~20 OBP stations are connected to cables off Kii Peninsula, and ~30 stations are located off Shikoku, both targeted to monitor tsunamis along the Nankai-Tonankai Trough[57]. The DONET/DONET2 OBPs detected several tsunamis of various sizes from the 2015 Torishima volcanic earthquake (Mw5.7) to the 2011 Tohoku Tsunami (Mw9.0). The S-net was installed after the 2011 Tohoku Tsunami along the Japan Trench. The S-net has 150 stations on 6 lines of cables with total lengths of 5,800 km.

Since July 2016, TEW systems have been developed using the offshore OBP data of S-net. For example, a near-field tsunami forecasting method has been developed based on tsunami waveform inversion[58]. First, the observed tsunami waveforms at OBP gauges are inverted for initial sea surface elevations without assuming fault geometry and earthquake magnitude[58]. Then, the coastal tsunami waveforms are forecasted by a linear combination of the estimated source and the pre-computed Green's functions[58]. This method, tFISH/RAPiD (tsunami Forecasting based on Inversion for initial sea-Surface Height/Real-time Automatic detection method for Permanent Displacement), has been further improved by using GNSS data[59]. The JMA has adopted the tFISH method for S-net data since 2019.

Another way of utilizing offshore tsunami data is tsunami data assimilation[60], which combines real-time tsunami data recorded at OBP gauges and numerical simulation to forecast coastal tsunami arrivals and nearshore heights without assuming the tsunami source. Real tsunami data recorded by OBP gauges in the Cascadia subduction zone were used to show that data assimilation made timely and accurate tsunami forecasting of the 2012 Haida Gwaii earthquake[61]. This approach was applied to the 2016 Fukushima earthquake[62], where tsunami data assimilation using OBP observations enabled the reconstruction of the assimilated wavefield and accurately predicted the tsunami waveforms at tide gauges before their arrivals[63].

TEWS were originally developed to estimate tsunami heights along the coast. These dense tsunami network can directly estimate tsunami source without estimation of earthquake fault. The direct tsunami source estimation greatly improved the accuracy of tsunami forecasts. Furthermore, it is now moving to real-time inundation forecasts based on the dense arrays of offshore observation data.

[H1] Tsunami Source and Generation

Advances in probabilistic tsunami hazard analysis (PTHA) incorporate the anticipated uncertainty associated with seismic occurrence and rupture characteristics of future megathrust events[64-69]. PTHA considers a comprehensive range of uncertainties in estimates of earthquake occurrence and rupture characteristics on tsunami waves[64]. Such probabilistic analysis contrasts with deterministic tsunami hazard analysis (DTHA), which is often performed for specific worst-case scenarios[70,71]. Earthquake occurrence modeling has the greatest impact on return period of tsunami [72]. In contrast, earthquake slip modeling has substantial effects on tsunami height and related tsunami hazard assessments[73,74], and statistical properties of slip models (for example, location, magnitude, and geometric slip distribution) have been considered in various studies worldwide[75-79]. In the following section, key aspects of earthquake occurrence and related rupture processes used in PTHA are summarized.

[H2] Earthquake occurrence

Important earthquake fault information for tsunamis is the length and width of the fault, its depth, and the amount of slip. In addition, the frequency of occurrence at each magnitude is also important information. Earthquake occurrence is one of the most influential elements in PTHA and involves substantial uncertainty[80] (Figure 4a-c).

The fundamental causes of large uncertainty in earthquake occurrence are that historical and instrumental tsunami records are short compared with recurrence periods of giant tsunamis[81], while paleotsunami records span a longer period but are very uncertain[82]. The lack of observed fault data and the short historical record make it difficult to estimate the macroscopic characteristics of the epicenter, the length and width of the fault, the amount of slip, and the statistical characteristics of the frequency of occurrence for PTHA. In other words, it is like not knowing the shape of a dice.

Although a time-independent homogeneous Poisson process (i.e. number of random events in a given time) is commonly adopted in PTHA, the occurrence rates of earthquakes in subduction zones are non-Poissonian and quasi-periodic[83-85]. Therefore, both physics-inspired occurrence models[86,87] and statistics-based renewal models[88] have been adopted. A renewal process can characterize the evolution of occurrence probability with time in terms of the inter-occurrence time distribution of earthquakes. It can account for the elapsed time since the previous event. There are several popular inter-arrival time distributions [89,90]. A homogeneous Poisson process corresponds to the exponential distribution with a constant occurrence rate. Typically, such an earthquake occurrence model is combined with a magnitude recurrence distribution which characterizes the uncertainty of earthquake magnitude when a major event occurs (Figure 4a). An recent advance of the time-space interaction model of earthquake occurrence includes the multi-segment time-dependent rupture model, represented by the multivariate Bernoulli model with renewal process-based probabilities[91].

[H2] Earthquake rupture process

Earthquake rupture is complex and is governed by pre-rupture stress and frictional conditions of the fault and trigger conditions of the rupture that are largely unknown and unobservable. The rupture of an earthquake is not uniform but heterogeneous. For example, the slip of a rupture may concentrate at one side. Although the energy is the same as a uniform rupture, the concentrated slip can induce stronger tsunami waves[92].

Through earthquake source inversions[93] or joint inversions, the spatiotemporal rupture process can be estimated by matching key features of simulated data with observations.

To characterize earthquake sources of future events, empirical scaling relationships of fault geometry and earthquake slip can be utilized[94-99] based on a series of historical earthquake source inversion or joint inversion data (Fig 4d).

To characterize the spatial distribution of earthquake slip, spectral analysis can be used to determine the wavenumber representation of earthquake slip heterogeneity[100-102], and generate a wide range of earthquake rupture scenarios (Fig 4c). Subsequently, the derived spectral model, such as the von Karman spectrum, can be used to generate stochastic earthquake slip distributions[101,102]. For stochastic source modeling, scaling relationships for spatial earthquake slip parameters are necessary[103,104]. To quantify the uncertainties of tsunami earthquake rupture, such stochastic source models have been used in various tsunami hazard studies that account for heterogeneous earthquake slips[75-79,105,106] (Fig 4c).

[H2] Rapid moment magnitude estimation

Rapid estimate of earthquake magnitude is essential for earthquake and tsunami hazard mitigations. However, accurately estimating the magnitude of a great earthquake within minutes after its occurrence remains a challenge. For example, as mentioned in previous sections, the 2004 Sumatra-Andaman was underestimated as magnitude 8.5 in the first hour, and the 2011 Tohoku earthquake was estimated magnitude 7.9 in the first 20-30 minutes. Traditional earthquake magnitude measuring methods, such as local magnitude M_L, body wave magnitude m_b, surface wave magnitude M_s, suffer from saturation problems when magnitude greater than 8.0. The moment magnitude M_w does not saturate but requires tens of minutes for long period signals to reach teleseismic stations (> 1000 km). W-phase inversion is an alternative method for promising estimate of moment magnitude with about 20 minutes[107] and has been adopted to real-time monitoring[108]. In addition to inversion approaches, empirical approaches methods are also used to estimate magnitudes of large earthquakes[109-112]. In the ideal case, the moment magnitude or comparable magnitude can be estimated as fast as 6-10 minutes[112].

Within tsunami source and generation, the earthquake occurrence and rupture process are very important for hazard assessment. On the other hand, rapid moment magnitude estimation is an important process for TEW system. As noted in Historical Giant Tsunamis, these techniques are closely related to observational data and have made significant progress since 2000, especially in the last decade.

[H1] Propagation and Inundation

The 2004 Indian Ocean Tsunami and the 2011 Tohoku Tsunami prompted the development of tsunami modeling for coastal to landward inundation processes. The damage caused by a tsunami cannot be estimated from the waveform of the tsunami to the coast. It is important to know how the water level and velocity of tsunami change as over the breakwater and onshore. Tsunami propagation in deep water can be described by linear or nonlinear shallow water equations, depending on the degree of nonlinearity of the tsunami waveform. Dispersion and other second-order effects are also important considerations in modeling long-distance tsunamis[113]. Wave dispersion means that waves of different periods travel at different phase speeds, for example, waves with shorter periods travel at slower phase speeds. After a certain distance traveling, short-period waves spatially fall behind long-period waves. Due to the complex nature of tsunami inundation, non-hydrostatic modeling is generally required for coastal to landward inundation processes if one is interested in details of tsunami interactions with complex bathymetry, topography, and structures.

[H2] Offshore propagation physics

Tsunami simulation with the incompressible long-wave assumption (Fig. 5a) accurately predicts tsunami arrival time in the near-field but can yield arrival times too early in the far-field. For example, after long-distance traveling, the observed tsunami arrival times were reported later than predicted during the 1960 Chile Tsunami and the 2004 Indian Ocean Tsunami, where 10-15 minutes delays were reported at distant stations with 19-20 hours travel time[114]. Furthermore, the 2010 Maule Tsunami and the 2011 Tohoku Tsunami had marked differences in their tsunami wave speeds between that observed by OBPGs and simulated values away from the source region[115]. Prediction errors in the waveform are also noted in the literature; while a leading trough (negative crest) is generally observed in the far-field, standard numerical models based on the nonlinear shallow water equations cannot recreate this characteristic[116].

To explain the systematic late arrivals of transoceanic tsunamis, additional physical factors have been introduced to solve these problems for the nonlinear shallow water equations, including elastic loading of the seafloor by tsunamis[116,117], compressible seawater[117-118], ocean density stratification[117,118], and gravitational potential change by tsunami motion[120]. All these factors reduce tsunami speed by up to 1.5 % in a 4 km deep ocean, which is equivalent to 18 minutes for a 20-hour travel time far-field tsunami[119,120]. The elastic loading of the seafloor and compressible seawater, accounting for around 1.1 % speed reduction in a 4-km-depth ocean, are the predominant factors. The reduced phase speed varies in different frequencies. For example, in a 4 km deep ocean, the maximum phase speed is in around 1000 second period and reduces for a larger or smaller period. With the arrival time discrepancy resolved, tsunami warning systems can accurately predict tsunami arrival time in the far-field. Furthermore, far-field tsunami data have been used to re-examine the recorded major tsunami events that suffer from insufficient near-field data[Error! Reference source not found.,121].

[H2] Nearshore and inundation physics

As a tsunami enters shallow water (Fig. 5b), the processes of shoaling and focussing control the wave speed and shape. In this area, tsunami current velocities and wave steepness grow quickly, leading to the generation of strong turbulence through bottom stress, interactions with complex bathymetry, and wave breaking; compared to modeling the offshore evolution of a tsunami, nearshore and onshore processes are more difficult to predict correctly. For example, for some tsunamis with very large incident crest heights, the leading crest can decompose into a series of much shorter waves (with periods of 10 seconds) through a process known as fission[124]. Tsunami-induced currents in the nearshore, taking into account of irregular bathymetry or coastal structures, are often characterized by large turbulent eddies or whirlpools[125]. Accurate modeling, while being sufficiently efficient with these chaotic features, is still an open research challenge[126].

The 2011 Tohoku Tsunami showed complex inundation behavior[127]. Especially in urban areas, land structures and their layouts had a substantial impact on the hydrodynamic characteristics of the tsunami (Fig. 5c). Even for the same inundation depth, the damage was different depending on the local topography and the layout of surrounding structures. In addition, coastal bathymetry and/or topography and shoreline complexity notably affected the probability of structural damage, with more complex topography resulting in higher damage rates[128-130]. These results indicate that it is difficult to represent the tsunami inundation characteristics of land areas using only inundation depth. Flow velocity and horizontal momentum flux should be included in addition to inundation depth[131,132].

Reproducing the inundation depth and flow velocity of tsunamis that run up to urban areas is important for future tsunami risk mitigation. However, the roughness model, typically dependent on the land-use category, cannot simulate the tsunami flow velocity in the urban area accurately. Therefore, it is necessary to evaluate the interactions between the structures for the inundation process in the numerical model[133]. To understand the characteristics of tsunami behavior in urban areas and to validate numerical models, physical experiments for tsunami inundations within complex building layouts have been conducted[134]. The physical model results and comparison with numerical models showed that the non-hydrostatic flow, including vertical velocity around the structures, cannot be neglected as it impacts the flow behind structures[135,136]. In addition, tsunami-generated debris can substantially affect the inundation behavior and the structural loads due to debris collision[137,138]. The challenges are that location, mass, moving speed, and impact angle of debris involve a great degree of uncertainty. Prediction of debris makes several times the difference in final location depending on these values.

n order to predict damage, it is most important to know quantitatively the water level and velocity of land side tsunami inundation process. For this reason, tsunami models are being developed for the propagation from offshore, very shallow water to land. Especially for tsunamis in urban areas, how to incorporate information on complex structures and buildings is becoming increasingly important; 3D city data will be very useful. Modeling of tsunami debris is even more difficult, and there are various efforts underway.

[H1] Long-term Risk Assessments

Based on a given tsunami condition, hardware or structure measures (such as sea walls) can reduce life, and asset and software or non-structural measures (such as evaluation, assessments and planning) can reduce life losses significantly. Long-term assessments of the tsunami will give a condition for soft and hardware countermeasures. However, a deterministic approach has limitation due to uncertainty of earthquake faults and tsunami modeling. The probabilistic tsunami risk assessment is one option to consider the variability of tsunami conditions for risk mitigation. Furthermore, comprehensive disaster prevention planning is important to maximize the effectiveness of tsunami countermeasures.

[H2] Probabilistic tsunami risk assessment

Modern PTHA frameworks described above can provide the basis for mitigating and controlling disaster risk exposures effectively in coastal areas. The key requirements are that those main uncertainties in earthquake occurrence, rupture process, and tsunami generation and propagation are quantified and incorporated into the assessments. In addition, epistemic uncertainty associated with PTHA elements should be accounted for by considering alternative models[139]. Outputs from such hazard assessments include site-specific tsunami hazard curves, which can be used for engineering design[140], and tsunami inundation maps at different return period levels, which can serve as the fundamental input to develop local and regional hazard mitigation plans[141].

Adopting and implementing PTHA approaches in a seismic region of interest offer two advantages. First, because of methodological similarity with probabilistic seismic hazard analysis[142], PTHA can be extended to probabilistic tsunami risk analysis and loss estimation[143] by integrating tsunami fragility models for probabilistic damage assessment[128, 129,144]. This integration has opened new avenues of research to develop and advance performance-based tsunami engineering (PBTE) methods, including analytical tsunami fragility modeling[145,146]. When combined with high-resolution inundation simulations, the effects of debris transport and collision on buildings can be included in tsunami vulnerability assessments[147]. Second, PTHA and PBTE approaches can be integrated with seismic counterparts and evolved into new multi-hazard methods[148-150]. For example, Fig. 6 shows joint shaking-tsunami risk maps for Kuroshio Town, which is located in southwestern Japan, facing the imminent threat due to future Nankai-Tonankai megathrust earthquakes and tsunamis[151,152]. With these new multi-hazard risk assessment tools, combined impacts due to ground shaking and tsunami can be evaluated more comprehensively. It is also important to emphasize that tsunami hazards and risks have interactions with other climate-related hazards, such as relative sea-level rise[153,154].

Earthquake-tsunami loss models serve as essential decision-support tools in designing structural risk mitigation measures and planning community-focused solutions, including evacuation planning and land-use planning. The multi-hazard loss models are also necessary for developing disaster risk financing tools, including insurance rate-making[155] and alternative risk transfer instruments, such as catastrophe bonds[156]. By integrating these key elements of earthquake-tsunami risk mitigation measures from a holistic risk management perspective, future resilience-based approaches for earthquakes and tsunamis have emerged[151]. They can be used to quantify and compare the benefits and costs associated with different alternatives, thereby promoting risk-informed decision-making in managing catastrophic earthquake-tsunami risks. Moreover, the new approaches can incorporate maintenance and inspection costs and environmental impacts from cradle-to-grave to further improve both the resilience and sustainability of society and the built environment for coastal communities.

[H2] Structural measure

Several countermeasures have been proposed and implemented to ameliorate the effects of tsunami inundation in communities and surrounding infrastructure. Hardware and structural countermeasures include coastal defense structures (dikes, seawalls, and breakwaters), nature-based systems (coastal forests), and building code requirements.

Coastal structures have long played an important role in coastal hazard mitigation[157]. While seawalls and dikes of sufficient elevation have been shown to play a protective role in tsunami mitigation[158], structural measures alone cannot prevent tsunami disasters. However, these structures can lead to a false sense of security for developments in inland areas[110]. Observations of damage to residential and other buildings following tsunami events have led to the development of fragility functions for predicting building vulnerability based on tsunami inundation height and flow velocity, among other parameters[129,131].

The 2011 Tohoku Tsunami caused substantial damage to coastal protection structures, including the Kamaishi breakwater, Ofunato Bay breakwater, and many coastal dikes in the Iwate, Miyagi, and Fukushima prefectures[159,47]. Following the Tohoku Tsunami, a new generation of coastal embankments was designed to better withstand overtopping forces, with the Japanese Government establishing a policy that structures should be built to ensure satisfactory performance. However, several have noted potential maintenance challenges associated with these newer, more resilient structures.

The effects of tsunami countermeasure structures on tsunami inundation and the resulting damages to community infrastructure can inform the design and location of these systems. Physical modeling[160] and numerical simulations[161-163], as well as Probabilistic Tsunami Hazard and Risk Analysis[164,165] can be used to evaluate the vulnerability of the existing building stock[162,166], and the efficacy of mitigation measures[160,167,168] under a performance-based or reliability framework[169,170]. For example, Syamsidik et al[168] evaluated the effects of installing an elevated roadway parallel to the coast in Banda Aceh, Indonesia, and found that the countermeasure could markedly reduce the tsunami inundation area and flow velocities. Tanaka et al[161] considered the combined effects of a coastal forest and sea wall on washout region reduction in the Tohoku and Kanto districts of Japan following the 2011 tsunami.

Nature-based solutions, including coastal forests, dunes, coral reefs, seagrasses, and greenbelts, or hybrid systems, such as tsunami mitigation parks [G], have also been proposed as a natural infrastructure approach to tsunami mitigation[171,172]. While coastal pine forests were observed during the 2011 Tohoku Tsunami to provide some mitigation through debris flow capture, particularly in inland zones, and reduced damage to dikes in some areas, other areas experienced complete destruction of coastal forests, which contributed to the impact of the tsunami through floating debris[172,173]. Osti et al.[174] noted the importance of coastal mangroves in tsunami disaster prevention. Indeed, coastal mangrove forests provided protection to communities during the 2004 Indian Ocean Tsunami in southeast India, Sri Lanka, and the Andaman Islands[175], and the Sulawesi earthquake and tsunami in Indonesia[176].

In addition to coastal defense structures and control forests, guidance for coastal defenses and buildings in tsunami inundation zones has been developed and modified to improve the robustness of buildings subject to tsunami loads[140,177]. The improvements in tsunami design codes aim to reduce the tsunami impact and damage based on a real experience that will provide an insight on tsunami safety and the resilience of coastal communities in the U.S. and elsewhere.

[H2] Non-structural measure

Life safety remains the highest priority in mitigating the tsunami disaster due to its catastrophic nature. The life safety issue is severe for near-field tsunamis for several reasons. First, there is a short time between the seismic event and the resulting inundation, typically tens of minutes, compared to several days of warning for hurricanes and typhoons. Second, evacuations will be self-initiated, relying on an individual's perception of risk and knowledge of the correct course of action. This can be problematic in areas where current generations of residents have not experienced major tsunamis. Third, the coastal population in some areas has a disproportionately larger population at risk due to age and socioeconomic status. Finally, life safety can be increased through a number of means, including structural measures, such as vertical evacuation facilities. Advances in evacuation modeling can help individuals better understand their risks to near-field tsunamis and determine the best travel routes. Further, these models can help communities to plan the locations of vertical evacuation structures, and assembly areas outside of inundation zones and to estimate required travel times throughout the tsunami inundation zone[178-181].

Tsunami evacuation models generally fall into two categories. Static models consider the optimized travel time out of the inundation zone. Typically, this least-cost-distance (LCD) approach can be used in a Geospatial Information System (GIS) framework[182] by incorporating land cover, slope, and other features to modify travel speeds[183]. These models can ingest large population data sets and can be implemented on a whole city-scale. However, they do not reflect factors in the tsunami inundation dynamics or human interactions. Dynamic models, such as Agent-Based Model (ABM), are more advanced in that they can capture the dynamics of tsunami inundation, interaction with the built environment, and complex human interactions. High-fidelity ABMs are generally run for smaller areas compared to LCD approaches.

The use of these ABMs can lead to counterintuitive results. For example, the shortest path might not provide the maximum risk reduction because tsunami inundation zones may exist along evacuation routes, or evacuees may be concentrated, causing traffic congestion[184]. Tsunami evacuation models have been used for case studies worldwide and can be used for evidence-driven resource allocation[185], to understand the impact of earthquake-induced debris on evacuation[186], and the dynamics of pedestrian-vehicle interaction[187]. Advances in computational efficiency might enable the increased use of ABMs combined with stochastic approaches, such as PTHA[181]. Fig. 7 illustrates how the ABM and stochastic tsunami modeling can be combined to evaluate the dynamic aspects of tsunami evacuations in Padang, Sumatra, Indonesia. However, similar to fire evacuation modeling, verification and validation of tsunami evacuation models remain a challenge. Even with extensive research over the last 20 years on the extreme events that occurred in the Indian Ocean, Chile, and Japan, there are relatively few validation data sets[187]. Data from evacuation drills, survivor surveys, expert judgment, or other means to qualitatively assess the models are needed.

[H2] Community-level disaster planning

A robust tsunami planning strategy requires higher-level government entities to develop and support legislation, policies, and guidance that can be implemented consistently at the local community levels. Effective planning involves multiple specialties at a local level, including personnel from: (i) local building and public works departments responsible for technical review and implementation of the mitigation process; (ii) land-use planning departments responsible for the community planning and development approval processes, and (iii) emergency management and response departments responsible for long-term implementation and sustainability of tsunami safety practices. Successful planning will also benefit from an accurate tsunami hazard analysis and a fair application of the risk analysis for different uses, such as the performance-based approach[188].

Land-use planning strategies for tsunami hazards exhibit differences between countries, but they do have similar components. In Japan, as an example, the 2011 Tohoku Tsunami triggered new mitigation and land-use planning practices through a new institution, Japan Reconstruction Agency[189]. In addition to newly engineered tsunami countermeasures, a two-tiered approach was created for residential and commercial development. Hazard areas at lower elevations (lower than the 1000-year inundation exceedance probability boundary) require land-use, mitigation, and evacuation strategies. Hazard areas at higher elevations focus on evacuation strategies. The process of implementing these guidelines has been delayed, in many cases, due to a lack of resources, emphasizing the need for early and continued funding for this work[190].

In the U.S., tsunami land-use and mitigation planning regulations and guidelines have been established in some states. For example, the State of Oregon was one of the first to develop restrictions on placing new development and structures critical to community resilience, including hospitals and police or fire stations, in tsunami hazard areas. Although the law restricting this development was repealed in 20XX, Oregon continuously supports structural and land-use strategies that protect communities and the public from tsunami hazards[191]. In addition, the State of California has utilized the Seismic Hazard Mapping Act of 1990 to create two-tiered tsunami hazard zones similar to the Japanese system, where assessments and mitigation strategies for new developments are to be implemented by local governmental agencies[192]. The U.S. National Tsunami Hazard Mitigation Program utilizes strategies developed by these states and creates guidance for mitigation and recovery planning for other state and local governmental entities[193]. Additionally, sustainable disaster education is also important to keep residential interests and knowledge of hazards and disaster risk reduction, and high tsunami awareness helps reducing the local tsunami fatality[194].

[H1] Summary and Future Perspectives

In this review, the overall picture of research for tsunami hazard is presented. both TEW and long-term assessment are important. For TEW enhanced observation networks and early warning systems have been developed and are being implemented in society. For long-term assessment, fault modeling for mega-trust subduction zones, tsunami propagation and inundation process modeling, and hazard assessment have been developed based on the latest observations and scientific research progress. Applications to hazard assessment and mitigation are showing realistic solutions.

First, a continuous archive of tsunami data by tsunami observation networks is important for modeling tsunami generation and propagation. Accumulation of observation data will help improve TEW accuracy and fault modeling. In addition, the development of temporal and spatial observations by satellites (for example, synthetic aperture radar, SAR) is also expected near future. The temporal and spatial observations lead directly to improved accuracy of initial tsunami value estimation. The TEWS has been developed to release rapid estimation of tsunami heights along the coast. However, real-time inundation forecasts are developing and need to improve both land-side tsunami modeling and 3D city data.

Second, understanding mega-earthquakes can improve the scaling laws for megathrust earthquake characteristics and improve probabilistic tsunami risk assessment[103]. It is also expected to improve tsunami inundation and damage risk modeling. However, there is a notable gap between the simulation of tsunami water levels up to the coastline, the calculation of inundation on land, and the assessments of damage to buildings and other structures. Onshore and land inundation simulations require information on structures such as breakwaters at the 1-meter scale. The inundation process is expected to improve with numerical model development and 3D city data. Furthermore, building damage assessment requires not only high-resolution age information, including building information but also fluid calculations that accurately solve fluid pressure. The prediction building destruction is required.

Further improvement of evacuation models, such as the Agent model[181], is needed to predict human damage and optimize evacuation routes. The development of probabilistic tsunami hazard models requires improvement not only in scaling laws for large earthquake characteristics but also in historical data to confirm the accuracy of the calculations. The development of tsunami hazard models requires further advancement of these unique technologies and a comprehensive compilation of historical data. Combining these disciplines will involve active collaboration among science, engineering, and social sciences.

[H1] References

1. Wirth, E. A., Sahakian, V. J., Wallace, L. M., & Melnick, D. The occurrence and hazards of great subduction zone earthquakes. *Nature Reviews Earth & Environment*, **3(2)**, 125-140. (2022).
2. Argus, D. F., Gordon, R. G., & DeMets, C. Geologically current motion of 56 plates relative to the no-net-rotation reference frame. Geochemistry, Geophysics, *Geosystems*, **12(11)**. (2011).
3. Ruiz, S., & Madariaga, R. Historical and recent large megathrust earthquakes in Chile. *Tectonophysics*, **733**, 37-56. (2018).
4. Ishizawa, T., Goto, K., Yokoyama, Y., & Goff, J. Dating tsunami deposits: Present knowledge and challenges. *Earth-Science Reviews*, **200**, 102971. https://doi.org/10.1016/j.earscirev.2019.102971. (2020).
5. Goff, J., Chagué-Goff, C., Nichol, S., Jaffe, B., & Dominey-Howes, D. Progress in palaeotsunami research. *Sedimentary Geology*, **243**, 70-88. https://doi.org/10.1016/j.sedgeo.2011.11.002. (2012).
6. Cisternas, M., Atwater, B.F., Torrejón, F., Sawai, Y., Machuca, G., Lagos, M., Eipert, A., Youlton, C., Salgado, I., Kamataki, T., & Shishikura M. Predecessors of the giant 1960 Chile earthquake. *Nature* **437**, 404–407 (2005).
7. Kanamori, H., & Cipar, J.J. Focal process of the great Chilean earthquake May 22, 1960. *Phys. Earth Planet. Inter.* **9**, 128–136 (1974).

8. Barrientos, S.E., & Ward, S.N. The 1960 Chile earthquake: inversion for slip distribution from surface deformation. *Geophys. J. Intl.* **103**, 589–598 (1990).
9. Fujii, Y., & Satake, K. Slip distribution and seismic moment of the 2010 and 1960 Chilean earthquakes inferred from tsunami waveforms and coastal geodetic data. *Pure Appl. Geophys.* **170**, 1493–1509 (2013).
10. Ho, T.C., Satake, K., Watada, S., & Fujii, Y. Source estimate for the 1960 Chile earthquake from joint inversion of geodetic and transoceanic tsunami data. *J. Geophys. Res. Solid Earth* **124** (2019).
11. Talley, H. C., & Cloud, W. K. United States Earthquakes, 1960. US Geological Survey (1984).
12. Fritz, H.M., Petroff, C.M., Catalán, P.A., Cienfuegos, R., Winckler, P., Kalligeris, N., Weiss, R., Barrientos, S.E., Meneses, G., Valderas-Bermejo, C., & Ebeling, C. Field survey of the 27 February 2010 Chile tsunami. *Pure Appl. Geophys.* **168**, 1989–2010 (2011).
13. Geist, E. L. Near-field tsunami edge waves and complex earthquake rupture. *Pure and Applied Geophysics*, **170(9)**, 1475-1491 (2013).
14. Satake, K., Rabinovich, A. B., Dominey-Howes, D., & Borrero, J. C. Introduction to “Historical and recent catastrophic tsunamis in the world: Volume II. Tsunamis from 1755 to 2010”. *Pure and Applied Geophysics*, **170(9)**, 1361-1367. (2013).
15. Cheung, K.F., Lay, T., Sun, L. et al. Tsunami size variability with rupture depth. *Nat. Geosci*. **15**, 33–36. https://doi.org/10.1038/s41561-021-00869-z. (2022)
16. Shearer, P., & Bürgmann, R. Lessons learned from the 2004 Sumatra-Andaman megathrust rupture. *Annual Review of Earth and Planetary Sciences*, **38(1)**, 103-131. (2010).
17. Park, J., Butler, R., Anderson, K., Berger, J., Benz, H., Davis, P. et al. Performance review of the global seismographic network for the Sumatra-Andaman megathrust earthquake. *Seismological Research Letters*, **76(3),** 331-343. (2005).
18. Stein, S., & Okal, E. A. Speed and size of the Sumatra earthquake. *Nature*, **434(7033)**, 581-582. (2005).
19. Lay, T., Kanamori, H., Ammon, C. J., Nettles, M., Ward, S. N., Aster, R. C., et al. The great Sumatra-Andaman earthquake of 26 December 2004. *Science*, **308(5725)**, 1127-1133. (2005).
20. Ishii, M., Shearer, P. M., Houston, H., & Vidale, J. E. Extent, duration and speed of the 2004 Sumatra–Andaman earthquake imaged by the Hi-Net array. *Nature*, **435(7044)**, 933-936. (2005).
21. Ammon, C. J., Ji, C., Thio, H. K., Robinson, D., Ni, S., Hjorleifsdottir, V., et al. Rupture process of the 2004 Sumatra-Andaman earthquake. *Science*, **308(5725)**, 1133-1139. (2005).
22. EM-DAT, Centre for Research on the Epidemiology of Disasters, Université catholique de Louvain, Brussels, Belgium (2022)
23. Lavigne, F., Paris, R., Grancher, D., Wassmer, P., Brunstein, D., Vautier, F. et al. Reconstruction of tsunami inland propagation on December 26, 2004 in Banda Aceh, Indonesia, through field investigations. *Pure and Applied Geophysics*, **166(1)**, 259-281. (2009).
24. National Geophysical Data Center. *NCEI/WDS Global Historical Tsunami Database*. NOAA, (2022)

25. Tsuji, Y., Namegaya, Y., Matsumoto, H., Iwasaki, S. I., Kanbua, W., Sriwichai, M., & Meesuk, V. The 2004 Indian tsunami in Thailand: Surveyed runup heights and tide gauge records. *Earth Planet. Sp.* **58**, 223–232 (2006).
26. Borrero, J. C., Synolakis, C. E., & Fritz, H. Northern Sumatra field survey after the December 2004 great Sumatra earthquake and Indian Ocean tsunami. *Earthquake Spectra*, **22(3_suppl)**, 93-104. (2006).
27. Goff, J., Liu, P.L., Higman, B., Morton, R., Jaffe, B.E., Fernando, H., Lynett, P., Fritz, H., Synolakis, C., & Fernando, S. Sri Lanka field survey after the December 2004 Indian Ocean tsunami. *Earthquake Spectra* **22**, 155–172 (2006).
28. Sheth, A., Sanyal, S., Jaiswal, A., & Gandhi, P. Effects of the December 2004 Indian Ocean tsunami on the Indian mainland. *Earthquake Spectra* **22**, 435–473 (2006).
29. Fritz, H.M., & Borrero, J.C. Somalia field survey after the December 2004 Indian Ocean tsunami. *Earthquake Spectra* **22**, 219–233 (2006).
30. Titov, V., Rabinovich, A.B., Mofjeld, H.O., Thomson, R.E., & González, F.I. The global reach of the 26 December 2004 Sumatra tsunami. *Science* **309**, 2045–2048 (2005).
31. Rabinovich, A.B., Titov, V., Moore, C., & Eblé, M. The 2004 Sumatra tsunami in the southeastern Pacific Ocean: new global insight from observations and modeling. *J. Geophys. Res. Oceans* **122**, 7992–8019 (2017).
32. Gower, J. Jason 1 detects the 26 December 2004 tsunami. *EOS*, **86**, 37–38 (2005).
33. Smith, W.H., Scharroo, R., Titov, V.V., Arcas, D., & Arbic, B.K. Satellite altimeters measure tsunami. *Oceanography* **18**, 11–13 (2005).
34. Arcas, D., & Titov, V. Sumatra tsunami: lessons from modeling. *Surveys Geophys.* **27**, 679–705 (2006).
35. Hirata, K., Satake, K., Tanioka, Y., Kuragano, T., Hasegawa, Y., Hayashi, Y., & Hamada, N. The 2004 Indian Ocean tsunami: Tsunami source model from satellite altimetry. *Earth Planet. Sp.* **58**, 195–201 (2006).
36. Fujii, Y., & Satake, K. Tsunami source of the 2004 Sumatra-Andaman Earthquake inferred from tide gauge and satellite data. *Bull. Seism. Soc. Am.* **97**, S192–S207 (2007).
37. Rudloff, A., Lauterjung, J., Münch, U., & Tinti, S. Preface "The GITEWS Project (German-Indonesian Tsunami Early Warning System)". *Natural Hazards and Earth System Sciences*, **9(4)**, 1381-1382. (2009).
38. Lay, T. A review of the rupture characteristics of the 2011 Tohoku-oki Mw 9.1 earthquake. *Tectonophysics*, **733**, 4-36. https://doi.org/10.1016/j.tecto.2017.09.022. (2018).
39. Uchida, N., & Bürgmann, R. A Decade of Lessons Learned from the 2011 Tohoku-Oki Earthquake. *Reviews of Geophysics*. **59(2)**, e2020RG000713. (2021).
40. Hayes, G. P., Earle, P. S., Benz, H. M., Wald, D. J., & Briggs, R. W. 88 Hours: The US Geological Survey national earthquake information center response to the 11 March 2011 Mw 9.0 Tohoku earthquake. *Seismological Research Letters*, **82(4)**, 481-493. (2011).
41. Ide, S., Baltay, A., & Beroza, G. C. Shallow dynamic overshoot and energetic deep rupture in the 2011 M w 9.0 Tohoku-Oki earthquake. *Science*, **332(6036)**, 1426-1429. (2011).

42. Lay, T., Ammon, C.J., Kanamori, H. et al. Possible large near-trench slip during the 2011 Mw 9.0 off the Pacific coast of Tohoku Earthquake. *Earth Planet Sp* **63**, 32 (2011). https://doi.org/10.5047/eps.2011.05.033
43. Hossen, M. J., Cummins, P. R., Roberts, S. G., & Allgeyer, S. Time reversal imaging of the tsunami source. *Pure and Applied Geophysics*, **172(3)**, 969-984. https://doi.org/10.1007/s00024-014-1014-5. (2015).
44. Mori, N., Takahashi, T., Yasuda, T., & Yanagisawa, H. Survey of 2011 Tohoku earthquake tsunami inundation and runup. *Geophys. Res. Lett.* **38**, L00G14 (2011).
45. Satake, K., & Fujii, Y. source models of the 2011 Tohoku earthquake and long-term forecast of large earthquakes. *Journal of Disaster Research*, **9(3)**, 272-280. (2014).
46. International Tsunami Survey Team (ITST) Post-Tsunami Survey Field Guide. 2nd Edition, *IOC Manuals and Guides* **37**, 2014
47. Suppasri, A., Shuto, N., Imamura, F., Koshimura, S., Mas, E., & Yalciner, A.C. Lessons learned from the 2011 Great East Japan Tsunami: Performance of tsunami countermeasures, coastal buildings, and tsunami evacuation in Japan. *Pure Appl. Geophys.* **170**, 993–1018 (2013).

48. Okal, E.A., The quest for wisdom: Lessons from seventeen tsunamis, 2004-2014, *Phil. Trans. Roy. Soc. London, Ser. A*, **373**, 20140370, 26 pp., (2015)
49. International Oceanographic Commission Technical Series. User's guide for the Pacific Tsunami Warning Center enhanced products for the Pacific Tsunami Warning System. In *International Oceanographic Commission Technical Series* **105**, (2015).
50. Whitmore, P.M., & Sokolowski, T.J. Predicting tsunami amplitudes along the North American coast from tsunamis generated in the northwest Pacific Ocean during tsunami warnings. *Sci. Tsunami Haz.* **14**, 147–166 (1996).
51. Synolakis, C.E., Bernard, E.N., Titov, T.T., Kânoğlu, U., & González, F.I. Standards, criteria, and procedures for NOAA evaluation of tsunami numerical models. *NOAA Technical Memorandum*. **OAR PMEL-135,** (NOAA/Pacific Marine Environmental Laboratory, 2007).
52. Aoi, S., Asano, Y., Kunugi, T., Kimura, T., Uehira, K., Takahashi, N., Ueda, H., Shiomi, K., Matsumoto, T., & Fujiwara, H. MOWLAS: NIED observation network for earthquake, tsunami and volcano. *Earth Planet. Sp.* **72**, 126 (2020).
53. Japan Meteorological Agency. Earthquakes and tsunamis – disaster prevention and mitigation efforts, *JMA brochure*, (2021).
54. Kato, T., Terada, Y., Nishimura, H., Nagai, T., & Koshimura, S. Tsunami records due to the 2010 Chile Earthquake observed by GPS buoys established along the Pacific coast of Japan. *Earth Planet. Sp.* **63**, e5–e8 (2011).
55. Kawai, H., Satoh, M., Kawaguchi, K., & Seki, K. Characteristics of the 2011 Tohoku tsunami waveform acquired around Japan by NOWPHAS equipment. *Coastal Enigeering. J.* **55**, 1350008 (2013).
56. Mulia, I. E., & Satake, K. Developments of tsunami observing systems in Japan. *Frontiers in Earth Science.* **8**, 145. (2020).
57. Kaneda, Y., Kawaguchi, K., Araki, E., Matsumoto, H., Nakamura, T., Kamiya, S., Ariyoshi, K., Hori, T., Baba, T., & Takahashi, N. Development and application of an advanced ocean floor network system for megathrust earthquakes and tsunamis. In *Seafloor observatories*, **643–662** (Springer, 2015).

58. Tsushima, H., Hino, R., Fujimoto, H., Tanioka, Y., & Imamura, F. Near-field tsunami forecasting from cabled ocean bottom pressure data. *J. Geophys. Res. Solid Earth* **114**, B06309 (2009).
59. Tsushima, H., Hino, R., Ohta, Y., Iinuma, T., & Miura, S. tFISH/RAPiD: Rapid improvement of near-field tsunami forecasting based on offshore tsunami data by incorporating onshore GNSS data. *Geophys. Res. Lett.* **41**, 3390–3397 (2014).
60. Maeda, T., Obara, K., Shinohara, M., Kanazawa, T., & Uehira, K. Successive estimation of a tsunami wavefield without earthquake source data: A data assimilation approach toward real-time tsunami forecasting. *Geophys. Res. Lett.* **42**, 7923–7932 (2015).
61. Gusman, A.R., Sheehan, A.F., Satake, K., Heidarzadeh, M., Mulia, I.E., & Maeda, T. Tsunami data assimilation of Cascadia seafloor pressure gauge records from the 2012 Haida Gwaii earthquake. *Geophys. Res. Lett.* **43**, 4189–4196 (2016).
62. Wang, Y., & Satake, K. Real-time tsunami data assimilation of S-net pressure gauge records during the 2016 Fukushima earthquake. *Seismol. Res. Lett.* **92**, 2145–2155. (2021).
63. Wang, Y., Tsushima, H., Satake, K. & Navarrete, P. Review on recent progress in near-field tsunami forecasting using offshore tsunami measurements: source inversion and data assimilation. *Pure Appl. Geophys.* (2021). https://doi.org/10.1007/s00024-021-02910-z
64. Mori, N., Goda, K., & Cox, D.T. Recent process in Probabilistic Tsunami Hazard Analysis (PTHA) for mega thrust subduction earthquakes. In *The 2011 Japan Earthquake and Tsunami: Reconstruction and Restoration* (eds Santiago-Fandiño, V., Sato, S., Maki, N., & Iuchi, K.) 469–485 (Springer, 2017).
65. Davies, G, Griffin, J., Løvholt, F., Glimsdal, S., Harbitz, C., Thio, H.K., Lorito, S., Basili, R., Selva, J., Geist, E., & Baptista, M.A. A global probabilistic tsunami hazard assessment from earthquake sources. *Geol. Soc. London Special Publication* **456**, 219–244 (2018).
66. Behrens, J., Løvholt, F., Jalayer, F., Lorito, S., Salgado-Gálvez, M.A., Sørensen, M., Abadie, S., Aguirre-Ayerbe, I., Aniel-Quiroga, I., Babeyko, A., & Baiguera, M. Probabilistic tsunami hazard and risk analysis: a review of research gaps. *Frontiers in Earth Science.* **9**, 114 (2021).
67. Geist, E. L., & Parsons, T. (2006). Probabilistic analysis of tsunami hazards. *Natural Hazards,* 37(3), 277-314.
68. Grezio, A., Babeyko, A., Baptista, M. A., Behrens, J., Costa, A., Davies, G.,...... & Thio, H. K. Probabilistic tsunami hazard analysis: multiple sources and global applications. *Reviews of Geophysics*, **55(4)**, 1158-1198 (2017).
69. Davies, G., & Griffin, J. Sensitivity of probabilistic tsunami hazard assessment to far-field earthquake slip complexity and rigidity depth-dependence: case study of Australia. *Pure and Applied Geophysics,* **177(3)**, 1521-1548 (2020).
70. Tinti S. and Armigliato A. The use of scenarios to evaluate the tsunami impact in southern Italy. *Mar Geol*. **199(3)**, 221–243 (2003).
71. Baptista M.A., Miranda J.M., Omira R., Antuns C. (2011) Potential inundation of Lisbon downtown by a 1755-like tsunami. *Natural Hazardsards Earth Syst Sci* **11**, 3319–3326.
72. Goda, K. Time-dependent probabilistic tsunami hazard analysis using stochastic rupture sources. Stoch. Environ. Res. Risk Assess. **33**, 341–358 (2019).

73. Geist, E.L. Complex earthquake rupture and local tsunamis. *J. Geophys. Res. Solid Earth* **107**, ESE-2 (2002).
74. Melgar, D., Williamson, A.L., & Salazar-Monroy, E.F. Differences between heterogenous and homogenous slip in regional tsunami hazards modelling. *Geophys. J. Intl.* **219**, 553–562 (2019).
75. Løvholt, F., Pedersen, G., Bazin, S., Kühn, D., Bredesen, R.E., & Harbitz, C. Stochastic analysis of tsunami runup due to heterogeneous coseismic slip and dispersion. *J. Geophys. Res. Oceans* **117**, C03047 (2012).
76. Davies, G., Horspool, N., & Miller, V. Tsunami inundation from heterogeneous earthquake slip distributions: Evaluation of synthetic source models. *J. Geophys. Res. Solid Earth* **120**, 6431–6451 (2015).
77. Mueller, C., Power, W., Fraser, S., & Wang, X. Effects of rupture complexity on local tsunami inundation: Implications for probabilistic tsunami hazard assessment by example. *J. Geophys. Res. Solid Earth* **120**, 488–502 (2015).
78. Park, H., & Cox, D.T. Probabilistic assessment of near-field tsunami hazards: Inundation depth, velocity, momentum flux, arrival time, and duration applied to Seaside, Oregon. *Coastal Enigeering.* **117**, 79–96 (2016).
79. Sepúlveda, I., Liu, P.L., & Grigoriu, M. Probabilistic tsunami hazard assessment in South China Sea with consideration of uncertain earthquake characteristics. *J. Geophys. Res. Solid Earth* **124**, 658–688 (2019).
80. Goda, K. Multi-hazard portfolio loss estimation for time-dependent shaking and tsunami hazards. *Frontiers in Earth Science*, **8**, 592444. (2020).
81. Behrens, J., Løvholt, F., Jalayer, F., Lorito, S., Salgado-Gálvez, M.A., Sørensen, M., Abadie, S., Aguirre-Ayerbe, I., Aniel-Quiroga, I., Babeyko, A., & Baiguera, M. Probabilistic tsunami hazard and risk analysis: a review of research gaps. *Frontiers in Earth Science.* **9**, 114 (2021).
82. Walton, M., Staisch, L., Dura, T., Pearl, J., Sherrod, B., Gomberg, J., Engelhart, S., Tréhu, A., Watt, J., Perkins, J., Witter, R., Bartlow, N., Goldfinger, C., Kelsey, H., Morey, A., Sahakian, V., Tobin, H., Wang, K., Wells, R., & Wirth, E. (2021). Toward an integrative geological and geophysical view of Cascadia Subduction zone earthquakes. *Annul Review of Earth and Planetary Sciences*, **49**, 367–398.
83. Ogata, Y. Estimating the hazard of rupture using uncertain occurrence times of paleoearthquakes. *J. Geophys. Res. Solid Earth* **104**, 17995–18014 (1999).
84. Sykes, L.R., & Menke, W. Repeat times of large earthquakes: Implications for earthquake mechanics and long-term prediction. *Bull. Seismol. Soc. Am.* **96**, 1569–1596 (2006).
85. Field EH, Jordan TH. Time - dependent renewal - model probabilities when date of last earthquake is unknown. *Bull. Seismol. Soc. Am.* **105**, 459–463 (2015).
86. Shimazaki, K., & Nakata, T. Time - predictable recurrence model for large earthquakes. *Geophys. Res. Lett.* **7**, 279–282 (1980).
87. Kiremidjian, A.S., & Anagnos, T. Stochastic slip-predictable model for earthquake occurrences. *Bull. Seismol. Soc. Am.* **74**, 739–755 (1984).
88. Cornell, A.C., & Winterstein, S.R. Temporal and magnitude dependence in earthquake recurrence models. *Bull. Seismol. Soc. Am.* **78**, 1522–1537 (1988).
89. Matthews, M.V., Ellsworth, W.L., & Reasenberg, P.A. A Brownian model for recurrent earthquakes. Bull. *Seismol. Soc. Am.* **92**, 2233–2250 (2002).
90. Abaimov, S.G., Turcotte, D.L., Shcherbakov, R., Rundle, J.B., Yakovlev, G., Goltz, C., & Newman, W.I. Earthquakes: Recurrence and interoccurrence

times. In *Earthquakes: Simulations, Sources and Tsunamis* (eds Tiampo, K.F., Weatherley, D.K., & Weinstein, S.A.), 777–795 (Birkhäuser Verlag, 2008).

91. Ceferino, L., Kiremidjian, A., & Deierlein, G. Probabilistic space - and time - interaction modeling of mainshock earthquake rupture occurrence. *Bull. Seismol. Soc. Am.* **110**, 2498–2518 (2020).
92. Melgar, D., Williamson, A. L., & Salazar-Monroy, E. F. Differences between heterogenous and homogenous slip in regional tsunami hazards modelling. *Geophysical Journal International*, **219(1)**, 553-562. (2019).
93. Mai, P.M., & Thingbaijam, K.K. SRCMOD: An online database of finite - fault rupture models. *Seismol. Res. Lett.* **85**, 1348–1357 (2014).
94. Blaser, L., Krüger, F., Ohrnberger, M., & Scherbaum, F. Scaling relations of earthquake source parameter estimates with special focus on subduction environment. *Bull. Seismol. Soc. Am.* **100**, 2914–2926 (2010).
95. Leonard, M. Earthquake fault scaling: Self-consistent relating of rupture length, width, average displacement, and moment release. *Bull. Seismol. Soc. Am.* **100**, 1971–1988 (2010).
96. Strasser, F.O., Arango, M.C., & Bommer, J.J. Scaling of the source dimensions of interface and intraslab subduction-zone earthquakes with moment magnitude. *Seismol. Res. Lett.* **81**, 941–950 (2010).
97. Murotani, S., Satake, K., & Fujii, Y. Scaling relations of seismic moment, rupture area, average slip, and asperity size for M~ 9 subduction - zone earthquakes. *Geophys. Res. Lett.* **40**, 5070–5074 (2013).
98. Thingbaijam, K.K., Mai, P.M., & Goda, K. New empirical earthquake source - scaling laws. *Bull. Seismol. Soc. Am.* **107**, 2225–2246 (2017).
99. Goda, K., & De Risi, R. Multi-hazard loss estimation for shaking and tsunami using stochastic rupture sources. *International journal of disaster risk reduction*. **28**, 539-554. (2018).
100. Herrero, A., & Bernard, P. A kinematic self-similar rupture process for earthquakes. *Bull. Seismol. Soc. Am.* **84**, 1216–1228 (1994).
101. Mai, P.M., & Beroza, G.C. A spatial random field model to characterize complexity in earthquake slip. *J. Geophys. Res. Solid Earth* **107**, ESE-10 (2002).
102. Goda, K., Mai, P.M., Yasuda, T., & Mori, N. Sensitivity of tsunami wave profiles and inundation simulations to earthquake slip and fault geometry for the 2011 Tohoku earthquake. *Earth Planet. Sp.* **66**, 1–20 (2014).
103. Goda, K., Yasuda, T., Mori, N., & Maruyama, T. New scaling relationships of earthquake source parameters for stochastic tsunami simulation. *Coastal Enigeering. J.* **58**, 1650010 (2016).
104. Melgar, D., & Hayes, G.P. The correlation lengths and hypocentral positions of great earthquakes. Bull. Seismol. Soc. Am. **109**, 2582–2593 (2019).
105. Li, L., Switzer, A. D., Chan, C. H., Wang, Y., Weiss, R., & Qiu, Q. (2016). How heterogeneous coseismic slip affects regional probabilistic tsunami hazard assessment: A case study in the South China Sea. *Journal of Geophysical Research: Solid Earth*, **121(8)**, 6250-6272.
106. Scala, A., Lorito, S., Romano, F., Murphy, S., Selva, J., Basili, R.,...... & Cirella, A. (2020). Effect of shallow slip amplification uncertainty on probabilistic tsunami hazard analysis in subduction zones: use of long-term balanced stochastic slip models. *Pure and Applied Geophysics*, **177(3)**, 1497-1520.
107. Kanamori, H., & Rivera, L. Source inversion of Wphase: speeding up seismic tsunami warning. *Geophysical Journal International*, **175(1),** 222-238. (2008).

108. Duputel, Z., Rivera, L., Kanamori, H., Hayes, G. P., Hirshorn, B., & Weinstein, S. Real-time W phase inversion during the 2011 off the Pacific coast of Tohoku Earthquake. *Earth, Planets and Space*, **63(7)**, 535-539. (2011).
109. Tsuboi, S., Abe, K., Takano, K., & Yamanaka, Y. Rapid determination of Mw from broadband P waveforms. *Bulletin of the Seismological Society of America*, **85(2)**, 606-613. (1995).
110. Lomax, A., & Michelini, A. Mwpd: a duration–amplitude procedure for rapid determination of earthquake magnitude and tsunamigenic potential from P waveforms. *Geophysical Journal International*, **176(1)**, 200-214. (2009).
111. Katsumata, A., Ueno, H., Aoki, S., Yoshida, Y., & Barrientos, S. Rapid magnitude determination from peak amplitudes at local stations. *Earth, Planets and Space*, **65(8)**, 843-853. (2013).
112. Wang, D., Kawakatsu, H., Zhuang, J., Mori, J., Maeda, T., Tsuruoka, H., & Zhao, X. Automated determination of magnitude and source length of large earthquakes using backprojection and P wave amplitudes. *Geophysical Research Letters*, **44(11)**, 5447-5456. (2017).
113. Glimsdal, S., Pedersen, G. K., Harbitz, C. B., & Løvholt, F. Dispersion of tsunamis: does it really matter?. *Natural Hazards and Earth System Sciences*, **13(6)**, 1507-1526. (2013).
114. Rabinovich, A.B., Woodworth, P.L. & Titov, V.V. Deep-sea observations and modeling of the 2004 Sumatra tsunami in Drake Passage. *Geophys. Res. Lett*. **38**, L16604, (2011).
115. Bai, Y., Yamazaki, Y., & Cheung, K.F. Interconnection of multi-scale standing waves across the Pacific Basin from the 2011 Tohoku Tsunami. *Ocean Modelling* **92**, 183–197 (2015).
116. Watada, S., S. Kusumoto, S. & and Satake, K. Travel time delay and initial phase reversal of distant tsunamis coupled with the self-gravitating elastic Earth, *J. Geophys. Res.*, **119** (5), 4287-4310 (2014).
117. Allgeyer, S., & Cummins, P. Numerical tsunami simulation including elastic loading and seawater density stratification. *Geophys. Res. Lett.* **41**, 2368–2375 (2014).
118. Watada, S. Tsunami speed variations in density-stratified compressible global oceans. *Geophys. Res. Lett.* **40**, 4001–4006 (2013).
119. Ho, T.-C., Satake, K., & Watada, S. Improved phase corrections for transoceanic tsunami data in spatial and temporal source estimation: Application to the 2011 Tohoku earthquake. *Journal of Geophysical Research: Solid Earth*, **122**, 10,155–10,175 (2017). https://doi.org/10.1002/2017JB015070
120. Baba, T., Allgeyer, S., Hossen, J., Cummins, P.R., Tsushima, H., Imai, K., Yamashita, K., & Kato, T. Accurate numerical simulation of the far-field tsunami caused by the 2011 Tohoku earthquake, including the effects of Boussinesq dispersion, seawater density stratification, elastic loading, and gravitational potential change. *Ocean Modelling* **111**, 46–54 (2017).
121. Carvajal, M., Cisternas, M., & Catalán, P.A. Source of the 1730 Chilean earthquake from historical records: Implications for the future tsunami hazard on the coast of Metropolitan Chile. *J. Geophys. Res. Solid Earth* **122**, 3648–3660 (2017).
122. NOAA Tohoku (East Coast of Honshu) Tsunami, March 11, 2011 Main Event Page: Global propagation animation of tsunami. *NOAA NCTR experimental research product* (2011).

123. Lynett, P.J. Precise prediction of coastal and overland flow dynamics: a grand challenge or a fool's errand. *J. Dis Res.* **11**, 615–623 (2016).
124. Matsuyama, M., Ikeno, M., Sakakiyama, T., & Takeda, T. A study of tsunami wave fission in an undistorted experiment. In *Tsunami and its Hazards in the Indian and Pacific Oceans*, Birkhäuser Basel, 617–631 (2007).
125. Borrero, J.C., Lynett, P.J., & Kalligeris, N. Tsunami currents in ports. *Phil. Trans. Royal Soc. A* **373**, 20140372 (2015).
126. Lynett, P.J., Gately, K., Wilson, R., Montoya, L., Arcas, D., Aytore, B., Bai, Y., Bricker, J.D., Castro, M.J., Cheung, K.F., & David, C.G. Inter-model analysis of tsunami-induced coastal currents. *Ocean Modelling* **114**, 14–32 (2017).
127. Mori, N., Cox, D.T., Yasuda, T., & Mase, H. Overview of the 2011 Tohoku earthquake tsunami damage and its relation to coastal protection along the Sanriku Coast. *Earthquake. Spectra* **29**, 127–143 (2013).
128. Suppasri, A., Koshimura, S., & Imamura, F. Developing tsunami fragility curves based on the satellite remote sensing and the numerical modeling of the 2004 Indian Ocean tsunami in Thailand. *Natural Hazards and Earth System Sciences.* **11**, 173–189 (2011).
129. Suppasri, A., Mas, E., Charvet, I., Gunasekera, R., Imai, K., Fukutani, Y., Abe, Y., & Imamura, F. Building damage characteristics based on surveyed data and fragility curves of the 2011 Great East Japan tsunami. *Natural Hazards*. **66**, 319–341 (2013).
130. Shimozono, T., & Sato, S. Coastal vulnerability analysis during tsunami-induced levee overflow and breaching by a high-resolution flood model. *Coastal Engineering.* **107**, 116–126 (2016).
131. Charvet, I., Suppasri, A., Kimura, H., Sugawara, D., & Imamura, F. A multivariate generalized linear tsunami fragility model for Kesennuma City based on maximum flow depths, velocities and debris impact, with evaluation of predictive accuracy. *Natural Hazards.* **79**, 2073–2099 (2015).
132. Attary, N., van de Lindt, J.W., Unnikrishnan, V., Barbosa, A.R., & Cox, D.T. Methodology for development of physics-based tsunami fragilities. *J. Struct. Eng*. **143**, 04016223 (2017).
133. Fukui, N., Prasetyo, A., & Mori, N. Numerical modeling of tsunami inundation using upscaled urban roughness parameterization. *Coastal Enigeering.***152**, 103534 (2019).
134. Fukui, N., Chida, Y., Zhang, Z., Yasuda, T., Ho, T.C., Kennedy, A., & Mori, N. Variations in building-resolving simulations of tsunami inundation in a coastal urban area. *J. Waterway Port Coast. Ocean Eng.* **148**, 04021044 (2022).
135. Park, H., Cox, D.T., Lynett, P.J., Wiebe, D.M., & Shin, S. Tsunami inundation modeling in constructed environments: A physical and numerical comparison of free-surface elevation, velocity, and momentum flux. *Coastal Enigeering*. **79**, 9–21 (2013).
136. Prasetyo, A., Tomiczek, T., Yasuda, T., Mori, N., & Mase, H. Characteristics of a tsunami wave using a hybrid tsunami generator. In *Coastal Structures and Solutions to Coastal Disasters 2015*, 164–175 (2017).
137. Como, A., & Mahmoud, H. Numerical evaluation of tsunami debris impact loading on wooden structural walls. *Eng. Struct.* **56**, 1249–1261 (2013).
138. Park, H., & Cox, D.T. Effects of advection on predicting construction debris for vulnerability assessment under multi-hazard earthquake and tsunami. *Coastal Engineering* **153**, 103541 (2019).

139. Miyashita, T., Mori, N., & Goda, K. Uncertainty of probabilistic tsunami hazard assessment of Zihuatanejo (Mexico) due to the representation of tsunami variability. *Coastal Engineering Journal* **62**, 413–428 (2020).
140. Chock, G.Y.K. Design for tsunami loads and effects in the ASCE 7-16 standard. *J. Struct. Eng.* **142**, 04016093 (2016).
141. Zamora, N., Catalán, P.A., Gubler, A., & Carvajal, M. Microzoning tsunami hazard by combining flow depths and arrival times. *Frontiers in Earth Science*. **8**, 591514 (2021).
142. Baker, J.W., Bradley, B., & Stafford, P. Seismic hazard and risk analysis. (Cambridge University Press, 2021).
143. Goda, K., & De Risi, R. Probabilistic tsunami loss estimation: stochastic earthquake scenario approach. *Earthquake Spectra* **33**, 1301–1323 (2017).
144. Tarbotton, C., Dall'Osso, F., Dominey-Howes, D., & Goff, J. The use of empirical vulnerability functions to assess the response of buildings to tsunami impact: comparative review and summary of best practice. *Earth-Sci. Rev.* **142**, 120–134 (2015).
145. Attary, N., Unnikrishnan, V.U., van de Lindt, J.W., Cox, D.T., & Barbosa, A.R. Performance-based tsunami engineering methodology for risk assessment of structures. *Eng. Struct.* **141**, 676–686 (2017).
146. Petrone, C., Rossetto, T., & Goda, K. Fragility assessment of a RC structure under tsunami actions via nonlinear static and dynamic analyses. *Eng. Struct*. **136**, 36–53 (2017).
147. Park, H., & Cox, D.T. Effects of advection on forecasting construction debris for vulnerability assessment under multi-hazard earthquake and tsunami. *Coastal Engineering*. **153**, 103541 (2019).
148. Kameshwar, S., Park, H., Alam, S., Farokhnia, K., Barbosa, A.R., Cox, D.T., & van de Lindt, J.W. Probabilistic decision-support framework for community resilience: Incorporating multi-hazards, infrastructure interdependencies, and target objectives in a Bayesian network. *Reliability Eng. Syst. Safety* **191**, 106568 (2019).
149. Park, H., Alam, M.S., Cox, D.T., Barbosa, A.R., & van de Lindt, J.W. Probabilistic seismic and tsunami damage analysis (PSTDA) of the Cascadia Subduction Zone applied to Seaside, Oregon. *Intl. J. Disaster Risk Red.* **35**, 101076 (2019).
150. Attary, N., van de Lindt, J.W., Barbosa, A.R., Cox, D.T., & Unnikrishnan, V.U. Performance-based tsunami engineering for risk assessment of structures subjected to multi-hazards: tsunami following earthquake. *J. Earthq. Eng.* **25**, 2065–2084 (2021).
151. Goda, K., De Risi, R., De Luca, F., Muhammad, A., Yasuda, T., and Mori, N. Multi-hazard earthquake-tsunami loss estimation of Kuroshio Town, Kochi Prefecture, Japan considering the Nankai-Tonankai megathrust rupture scenarios. *Intl. J. Disaster Risk Red.* **54**, 102050 (2021).
152. Goda, K., Risi, R. D., Luca, F. D., Muhammad, A., Yasuda, T., & Mori, N. Earthquake-Tsunami Risk Assessment and Critical Multi-hazard Loss Scenarios: A Case Study in Japan Under the Nankai-Tonankai Mega-Thrust. In *Engineering for Extremes* (pp. 235-254). Springer, Cham. (2022).
153. Li, L., Switzer, A. D., Wang, Y., Chan, C. H., Qiu, Q., & Weiss, R. (2018). A modest 0.5-m rise in sea level will double the tsunami hazard in Macau. *Science Advances*, **4(8)**, eaat1180.

154. Alhamid, A.K., Akiyama, M., Ishibashi, H., Aoki, K., Koshimura, S., & Frangopol, D.M. (2022). Framework for probabilistic tsunami hazard assessment considering the effects of sea-level rise due to climate change. *Structural Safety*, **94**, 102152.
155. Song, J., & Goda, K. Influence of elevation data resolution on tsunami loss estimation and insurance rate-making. *Frontiers in Earth Science*. **7**, 246 (2019).
156. Goda, K. Multi-hazard parametric catastrophe bond trigger design for subduction earthquakes and tsunamis. *Earthquake Spectra* **37**, 1827–1848 (2021).
157. Shuto, N., & Fujima, K. Review: A short history of tsunami research and countermeasures in Japan. *Proc. Japan. Acad., Ser. B* **85**, 267-275 (2009).
158. Koshimura, S., & Shuto, N. Response to the 2011 Great East Japan Earthquake and Tsunami disaster. *Phil. Trans. Royal Soc. A* **373**, 20140373. (2015).
159. Kato, F., Suwa, Y., Watanabe, K., & Hatogai, S. Mechanisms of coastal dike failure induced by the Great East Japan Earthquake Tsunami. *Coastal Engineering Proc.* **33**, (2012).
160. Chen, J., Jiang, C., Yang, W. , and Xiao, G. 2016. Laboratory study on protection of tsunami-induced scour by offshore breakwaters, *Natural Hazards*, **81**, 1229–1247, 2016.
161. Tanaka, N., Yasuda, S., Iimura, K., Yagisawa, J. 2014. Combined effects of coastal forest and sea embankment on reducing the washout region of houses in the Great East Japan tsunami. *J. Hydro-environmental Research*, **8(3)** 270-280. Doi: 10.1016/j.jher.2013.10.001
162. Park, H. Cox, D.T., and Barbosa, A.R. 2017. Comparison of inundation depth and momentum flux based fragilities for probabilistic tsunami damage assessment and uncertainty analysis. *Coastal Engineering*, **122** 10-26 (2017). Doi: 10.1016/j.coastaleng.2017.01.008
163. Guler, H. G., Baykal, C., Arikawa, T., and Yalciner, A. C. 2018. Numerical assessment of tsunami attack on a rubble mound breakwater using OpenFOAM, Appl. *Ocean Res.*, **72**, 76–91, 2018
164. Jelínek, R., and Krausmann, E. 2008. Approaches to tsunami risk assessment. *JRC Sci. Tech. Rep.* **48713**, 112. doi:10.4324/9781351140843-3
165. Behrens J, Løvholt F, Jalayer F, Lorito S, Salgado-Gálvez MA, Sørensen M, Abadie S, Aguirre-Ayerbe I, Aniel-Quiroga I, Babeyko A, Baiguera M, Basili R, Belliazzi S, Grezio A, Johnson K, Murphy S, Paris R, Rafliana I, De Risi R, Rossetto T, Selva J, Taroni M, Del Zoppo M, Armigliato A, Bureš V, Cech P, Cecioni C, Christodoulides P, Davies G, Dias F, Bayraktar HB, González M, Gritsevich M, Guillas S, Harbitz CB, Kânoğlu U, Macías J, Papadopoulos GA, Polet J, Romano F, Salamon A, Scala A, Stepinac M, Tappin DR, Thio HK, Tonini R, Triantafyllou I, Ulrich T, Varini E, Volpe M and Vyhmeister E. 2021 Probabilistic Tsunami Hazard and Risk Analysis: A Review of Research Gaps. *Frontiers in Earth Science*. **9:628772.** doi: 10.3389/feart.2021.628772
166. Salgado-Gálvez, M. A., Zuloaga-Romero, D., Bernal, G. A., Mora, M. G., and Cardona, O.-D. 2014. Fully probabilistic seismic risk assessment considering local site effects for the portfolio of buildings in Medellín, Colombia. *Bull. Earthq. Eng.* **12 (2)**, 671–695. doi:10.1007/s10518-013-9550-4
167. Ozer, S. C., Yalciner, A. C., Zaytsev, A., Suppasri A., and Imamura, F. 2015. Investigation of Hydrodynamic Parameters and the Effects of Breakwaters

During the 2011 Great East Japan Tsunami in Kamaishi Bay, *Pure Appl. Geophys*., **172**, 3473–3491, 2015

168. Syamsidik, Tursina, Suppasri, A., Al'ala, M., Luthfi, M., and Comfort, L.K. 2019. Assessing the tsunami mitigation effectiveness of the planned Banda Aceh Outer Ring Road (BORR), Indonesia. *Natural Hazards Earth Syst. Sci.* **19**, 299-312.
169. Chock, G., Yu, G., Thio, H. K., and Lynett, P. J. 2016. Target structural reliability analysis for tsunami hydrodynamic loads of the ASCE 7 standard. *J. Struct. Eng.* **142**, 04016092–4016112. doi:10.1061/(ASCE)ST10.1061/(asce)st.1943-541x.0001499
170. Akiyama, M., Frangopol, D. M., and Ishibashi, H. 2020. Toward life-cycle reliability-, risk- and resilience-based design and assessment of bridges and bridge networks under independent and interacting hazards: emphasis on earthquake, tsunami and corrosion. *Struct. Infrastruct. Eng.* **16(1)**, 26–50. doi:10.1080/15732479.2019.1604770
171. Muhari, A., Diposaptono, S., & Imamura, F. Toward an Integrated Tsunami Disaster Mitigation: Lessons Learned from Previous Tsunami Events in Indonesia. *J. Nat. Disaster Sci*. **29**, 13–19 (2007).
172. Lunghino, B., Santiago Tate, A.F., Mazereeuw, M., Muhari, A., Giraldo, F.X., Marras, S., & Suckale, J. The protective benefits of tsunami mitigation parks and ramifications for their strategic design. *PNAS* **117**, 10740–10745 (2020).
173. Tanaka, N. Effectiveness and limitations of coastal forest in large tsunami: Conditions of Japanese pine trees on coastal sand dunes in tsunami caused by Great East Japan Earthquake. *J. Japan Soc. Civil Eng. Ser. B1*. **68**, (2012).
174. Osti, R., Tanaka, S., & Tokioka, T. The importance of mangrove forest in tsunami disaster mitigation. *Disasters* **33**, 203–213. (2009).
175. Danielsen, F., Sørenson, M.K., Olwig, M.F., Selvam, V., Parish, F., Burgess, N.D., Hiraishi, T., Karunagaran, V.M., Rasmussen, M.S., Hansen, L.B., Quarto, A., & Suryadiputra, N. The Asian tsunami: A protective role for coastal vegetation. *Science* **310**, 643 (2005).
176. Goda, K., Mori, N., Yasuda, T., Prasetyo, A., Muhammad, A., & Tsujio, D. Cascading geological hazards and risks of the 2018 Sulawesi Indonesia earthquake and sensitivity analysis of tsunami inundation simulations. *Frontiers in Earth Science*. **7**, 261 (2019).
177. American Society of Civil Engineers. Minimum design loads and associated criteria for buildings and other structures. *ASCE-SEI* 7-22 (2022).
178. Taubenböck, H., Goseberg, N., Setiadi, N., Lämmel, G., Moder, F., Oczipka, M., Klüpfel, H., Wahl, R., Schlurmann, T., Strunz, G., Birkmann, J., Nagel, K., Siegert, F., Lehmann, F., Dech, S., Gress, A., & Klein, R. "Last-Mile" preparation for a potential disaster – Interdisciplinary approach towards tsunami early warning and an evacuation information system for the coastal city of Padang, Indonesia. *Natural Hazards and Earth System Sciences*. **9**, 1509–1528 (2009).
179. Mas, E., Koshimura, S., Imamura, F., Suppasri, A., Muhari, A., & Adriano, B. Recent advances in agent-based tsunami evacuation simulations: Case studies in Indonesia, Thailand, Japan and Peru. *Pure Appl. Geophys.* **172**, 3409–3424 (2015).
180. Wood, N.J., Jones, J., Schmidtlein, M.C., Schelling, J., & Frazier, T. Pedestrian flow-path modeling to support tsunami evacuation and disaster relief planning in the U.S. Pacific Northwest," *Intl. J. Disaster Risk Red.* **18**, 41–55 (2016).

181. Muhammad, A., De Risi, R., De Luca, F., Mori, N., Yasuda, T., & Goda, K. Are current tsunami evacuation approaches safe enough? *Stoch. Environ. Res. Risk Assess.* **35**, 759–779 (2021).
182. Wood, N.J., & Schmidtlein, M.C. Anisotropic path modeling to assess pedestrian evacuation potential from Cascadia-related tsunamis in the US Pacific Northwest. *Natural Hazards.* **62**, 275–300 (2012).
183. Schmidtlein, M.C., & Wood, N.J. Sensitivity of tsunami evacuation modeling to direction and land cover assumptions. *Appl. Geography* **56**, 154–163 (2015).
184. Kitamura, F., Inazu, D., Ikeya, T., & Okayasu, A. An allocating method of tsunami evacuation routes and refuges for minimizing expected casualties. *Intl. J. Disaster Risk Red.* **45**, 101519 (2020).
185. Mostafizi, A., Wang, H., Dong, S., Cox, D.T., & Cramer, L. Agent-based tsunami evacuation modeling with unplanned network disruptions for evidence-driven resource allocation and planning strategies. *Natural Hazards.* **88**, 1347–1372 (2017).
186. Castro, S., Poulos, A., Herrera, J.C., & de la Llera, J.C. Modeling the impact of earthquake-induced debris on tsunami evacuation times of coastal cities. *Earthquake Spectra* **35**, 137–158 (2019).
187. Makinoshima, F., Imamura, F., & Abe, Y. Behavior from tsunami recorded in the multimedia sources at Kesennuma City in the 2011 Tohoku Tsunami and its simulation by using the evacuation model with pedestrian-car interaction. *Coast. Eng. J.* **8**, 1640023 (2018).
188. Wilson, R., Thio, H.K., Johnson, L., McCrink, T., Ewing, L., Street, J., Miller, K., LaDuke, Y., Wood, N., & Peters, J. Development and use of probabilistic tsunami hazard analysis maps in California. *Proc. 11th Nat. Conf. Earthq. Eng*. (2018).
189. Japan Reconstruction Agency, 2016, Basic guidelines for reconstruction in response to the Great East Japan Earthquake in the “Reconstruction and Revitalization Period;” produced by the Japan Reconstruction Agency, 18 p.
190. Cosson, C. “Build Back Better”: Between public policy and local implementation, the challenges in Tohoku’s reconstruction. *Architecture Urban Plan.* **16**, 1-4. (2020).
191. Oregon Seismic Safety Policy Advisory Council. Tsunami resilience on the Oregon coast. *OSSPAC Publication* 21-01 (2021).
192. California Geological Survey. Guidelines for evaluating and mitigation tsunami hazards in *California. California Geological Survey Special Publication* 127 (2022).
193. National Tsunami Hazard Mitigation Program. National tsunami hazard mitigation program strategic plan: 2018-2023. (2018).
194. Esteban, M., Tsimopoulou, V., Mikami, T., Yun, N. Y., Suppasri, A., & Shibayama, T. Recent tsunamis events and preparedness: Development of tsunami awareness in Indonesia, Chile and Japan. *International Journal of Disaster Risk Reduction*, 5, 84-97. (2013).

Acknowledgements

NM acknowledges funding from Grant-in-Aid for Scientific Research (KAKENHI) 20KK0095 and 21H04508, JST/JICA SATREPS Indonesia, DPRI-ERI Research Fund 2019-K-01 and 2021-K-01. K.G acknowledges funding from Canada Research Chair program (950-232015) and the Natural Sciences and Engineering Research Council Discovery Grant (RGPIN-2019-05898) . P.A.C acknowledges funding from ANID; Chile Centro de Investigación para la Gestión Integrada del Riesgo de Desastres (CIGIDEN) ANID/FONDAP/15110017, and Centro Científico Tecnológico de Valparaíso; ANID PIA/APOYO AFB180002.

Author Contributions

N.M. and K.G. led the writing and revision of the manuscript, with input and contributions from K.S, D.T, P.A.C, F.I., T.T., P.L., T.M., A.M., V.T., T.C.H., and R.W. All authors made substantial contributions to the discussion of content.

Competing Interests

The authors declare no competing interests.

Peer review information

Nature Reviews Earth & Environment thanks [Referee#1 name], [Referee#2 name] and the other, anonymous, reviewer(s) for their contribution to the peer review of this work.

Publisher's note

Supplementary information

Supplementary information is available for this paper at https://doi.org/10.1038/s415XX-XXX-XXXX-X

Related links

GDC/WDS Global Historical Tsunami Database – https://www.ngdc.noaa.gov/hazard/tsu_db.shtml

EM-DAT, CRED / UCLouvain, Brussels, Belgium https://www.emdat.be/

Japan Meteorological Agency. Earthquakes and tsunamis – disaster prevention and mitigation efforts. http://www.jma.go.jp/jma/kishou/books/jishintsunami/jishintsunami.pdf

NOAA Tohoku (East Coast of Honshu) Tsunami, March 11, 2011 Main Event Page: Global propagation animation of tsunami. Retrieved from https://nctr.pmel.noaa.gov/honshu20110311/

Figure Captions

Fig. 1 | Overview of tsunami generation, propagation, early warning, and long-term assessment. a| Earthquake-triggered tsunamis are generated by displacement at the seafloor by a fault rupture. Ocean bottom sensors, tsunami buoys and onshore seismic networks detect the earthquake and any resulting tsunami. **b|** A typical representation of a subduction zone. Shallow (~<15 km) rupture of the updip region of the subducting plate or of splay faults within the accretionary wedge can cause large amounts of slip on the fault and displacement of the seafloor. **c|** Information from monitoring networks and patterns from historical events are fed into early warning systems and long-term risk assessments. The observation relates the tsunami early warning and the long-term assessment.

Fig. 2 | Historical giant tsunamis. Tsunamis are usually generated by seismic slip during an earthquake (circles), but they can also be generated from other sources such as volcanic eruptions, landslides or rockfalls (triangles). Both types of tsunamis can cause numerous casualties and substantial destruction. Data from the NOAA-NGDC Tsunami Database. Major historical events occur in the subduction zone mainly along the Pacific Ocean.

Fig. 3 | Ocean bottom pressure monitoring network in Japan. OBP gauges monitor ocean bottom pressure and convert it to sea-level heights, so that tsunamis can be detected in the deep ocean. More than 200 OBP gauges (yellow dots) are connected by seafloor cables (bold black line) around the Japan Trench. The two main OBP systems are DONET and S-net[28,56] and 18 GPS bouys are NOWPHAS. The high-resolution, high-sampling data are sent to monitoring authorities in real-time[56]. A very dense tsunami observation network was established for the next earthquake and tsunami after 2011.

Fig. 4 | Components of earthquake occurrence and rupture models. a| Elements of a renewal-process-based earthquake occurrence model. A renewal process distinguishes the probability distributions for the first and subsequent earthquake events based on the elapsed time since the last major event. **b|** An earthquake magnitude model can be represented by a Gutenberg-Richter model [G], where the overall occurrence rate for major events and the relative distribution of earthquake magnitude is determined from statistical analysis of regional seismicity or by a characteristic magnitude model with uniform marginal distribution. **c|** Stochastic event catalogs can be generated over a specified time duration by combining simulated earthquake occurrence times (panel **a**) and magnitudes (panel **b**). **d|** Earthquake scaling relationships for fault length and mean earthquake slip are used to simulate various earthquake source parameters. **e|** stochastic earthquake source models use the earthquake parameters simulated from the scaling relationships to synthesize heterogeneous earthquake slip distributions and a wide range of rupture scenarios. As examples, three realizations of stochastic earthquake slip distributions for an Mw9 event off the Tohoku region of Japan are shown. Both the stochastic events (panel **c**) and the stochastic source models (panel **e**) can be combined and used in probabilistic tsunami hazard analysis (PTHA).

Fig. 5 | Hierarchy of length-scales for tsunami simulations. a| An example of global-scale tsunami propagation modeling (taken from NOAA[122]) with resolution typically in excess of 1 km. **b|** A nearshore domain tsunami propagation model with 10 km^2 coverage and resolutions near 10 m. **c|** A structure-resolving overland flow simulation[123], with resolutions of 1 m or less. Panel c adapted with permission from ref. [123] Building and street scale tsunami assessments require simulations starting at the 1000 km scale and going down to the 1 m scale.

Fig. 6 | Multi-hazard assessments combine risks from earthquake and tsunami hazards. An example of a probabilistic shaking-tsunami risk assessment for Kuroshio Town, Kochi Prefecture, Japan. **a|** stochastic source modeling, **b|** shaking hazard footprint, **c|** tsunami hazard footprint, **d|** shaking fragility, **e|** tsunami fragility, **f|** shaking damage ratio, **g|** tsunami damage ratio, and **h|** combined damage ratio. Starting from the fault model (a), the probability of damage (f, g) for each building is calculated based on the damage curves (d, e) from the shaking intensity (b) and tsunami depth (c), respectively, and the total damage (h) is summarized by both damages.

Fig. 7 | Evacuation assessments for urban environments under different tsunami scenarios. Tsunami evacuation simulations are shown for Padang, Sumatra, Indonesia, which is subject to potential tsunami threats from the Sunda-Mentawai subduction zone. **a|** agent-based evacuation model, **b|** stochastic tsunami simulations, and **c|** tsunami evacuation simulations. In the agent-based model, evacuation simulations are performed based on tsunami simulations (b) from evacuation routes (a-left) and human arrangements (a-right) to evaluate the ease of evacuation and bottlenecks (c).

Glossary

DART - real-time tsunami monitoring systems by NOAA

DONET - Deep Ocean-floor Network system for Earthquakes and Tsunamis

Edge waves – long-wave propagate along the coast

Far-field tsunami - tsunami occurs far from the location of target (more than 1000 km) without seismic shake

Gutenberg-Richter model – empirical relation to estimate frequency of earthquake

Hazard – intensity of natural phenomenon

Long-term assessment – estimation of hazard intensity and frequency based on historical data or model results

Magnitude – a measure of an earthquake's size or strength)

Megathrust earthquake tsunami – tsunami occurs at the subduction zone

MEXT – The Japanese Ministry of Education, Culture, Sports, Science and Technology

Moment magnitude (Mw) - a measure of an earthquake's magnitude based on its seismic moment.

Near-field tsunami – tsunami occurs near the location of target with seismic shake

Paleotsunami - tsunamis that occurred prior to historical records or for which there are no written observations (as defined by the International Tsunami Information Center).

Probabilistic tsunami hazard assessments – probabilistic estimation of tsunami intensity and frequency

Risk – combination of hazard, exposure and vulnerability

S-net - Seafloor observation network for earthquakes and tsunamis along the Japan Trench

ShakeAlert system - earthquake early warning system developed by USGS

Subduction zone – collision between oceanic lithosphere and continental crust

Tsunami early warning – real time tsunami prediction based on seismic or tsunami observation data

Tsunami trace height - the elevation with respect to sea level of tsunami traces, such as debris or flow markers in structures which correspond to the run-up or inundation height

Tsunami mitigation parks – a space to reduce tsunami forces

Fig 1

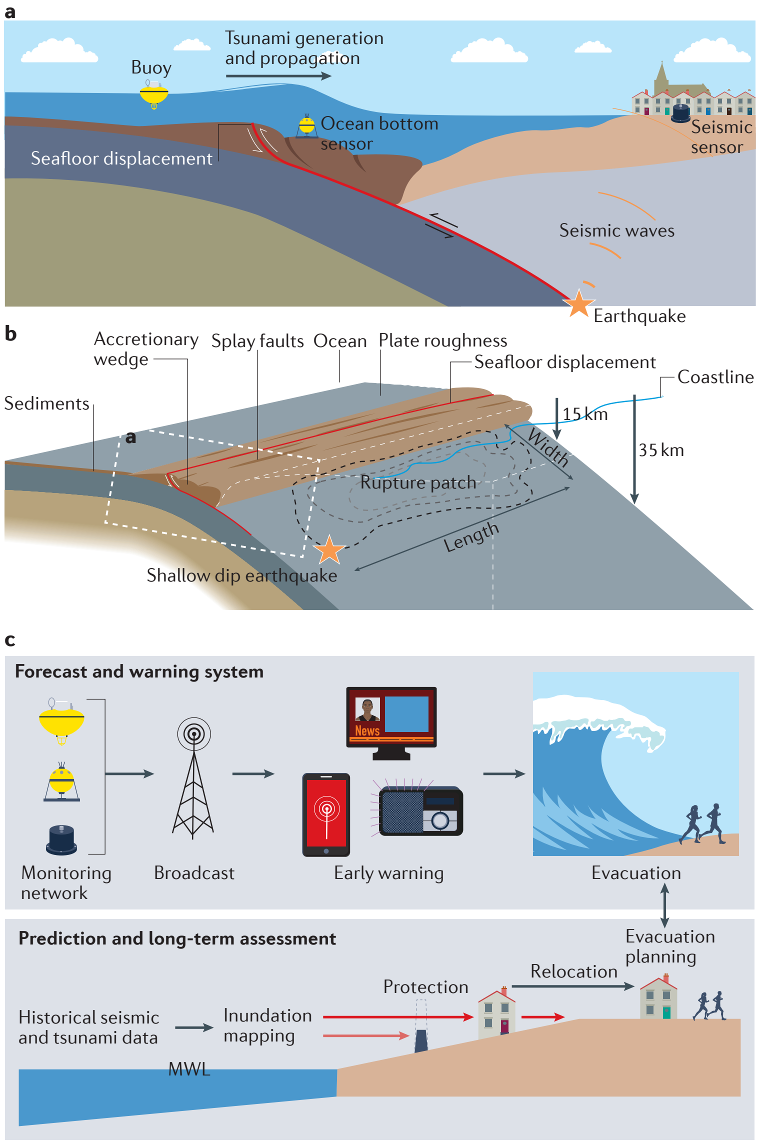
a
Tsunami generation
and propagation
Buoy
Ocean bottom
sensor
Seafloor displacement
Seismic
sensor
Seismic waves
Earthquake
b
Accretionary
wedge
Splay faults
Ocean
Plate roughness
Seafloor displacement
Coastline
Sediments
a
15 km
35 km
Width
Rupture patch
Length
Shallow dip earthquake
c
Forecast and warning system
News
Monitoring
network
Broadcast
Early warning
Evacuation
Prediction and long-term assessment
Evacuation
planning
Relocation
Protection
Historical seismic
and tsunami data
Inundation
mapping
MWL

Fig 2

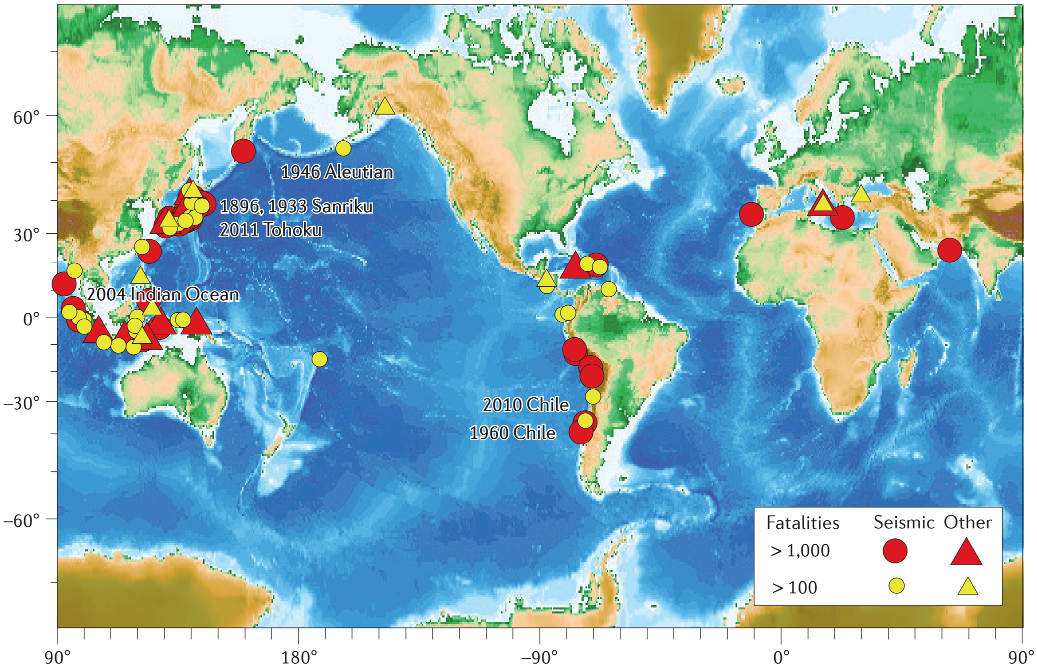
60°
30°
0°
−30°
−60°
90°
180°
−90°
0°
90°
1946 Aleutian
1896, 1933 Sanriku
2011 Tohoku
2004 Indian Ocean
2010 Chile
1960 Chile
Fatalities
Seismic
Other
> 1,000
> 100

Fig 3

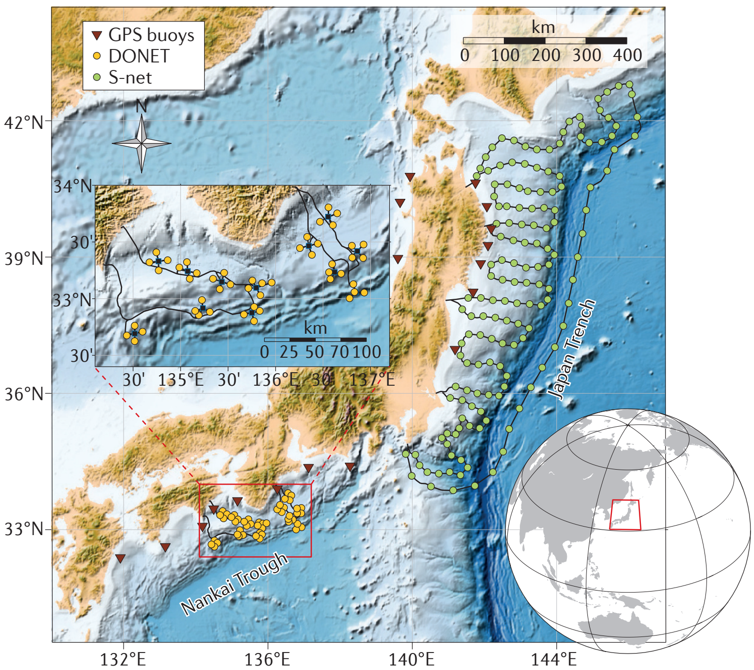
GPS buoys
DONET
S-net
km
0 100 200 300 400
42°N
39°N
36°N
33°N
132°E
136°E
140°E
144°E
N
34°N
30'
33°N
30'
30' 135°E 30' 136°E 30' 137°E
km
0 25 50 70 100
Japan Trench
Nankai Trough

Fig 4

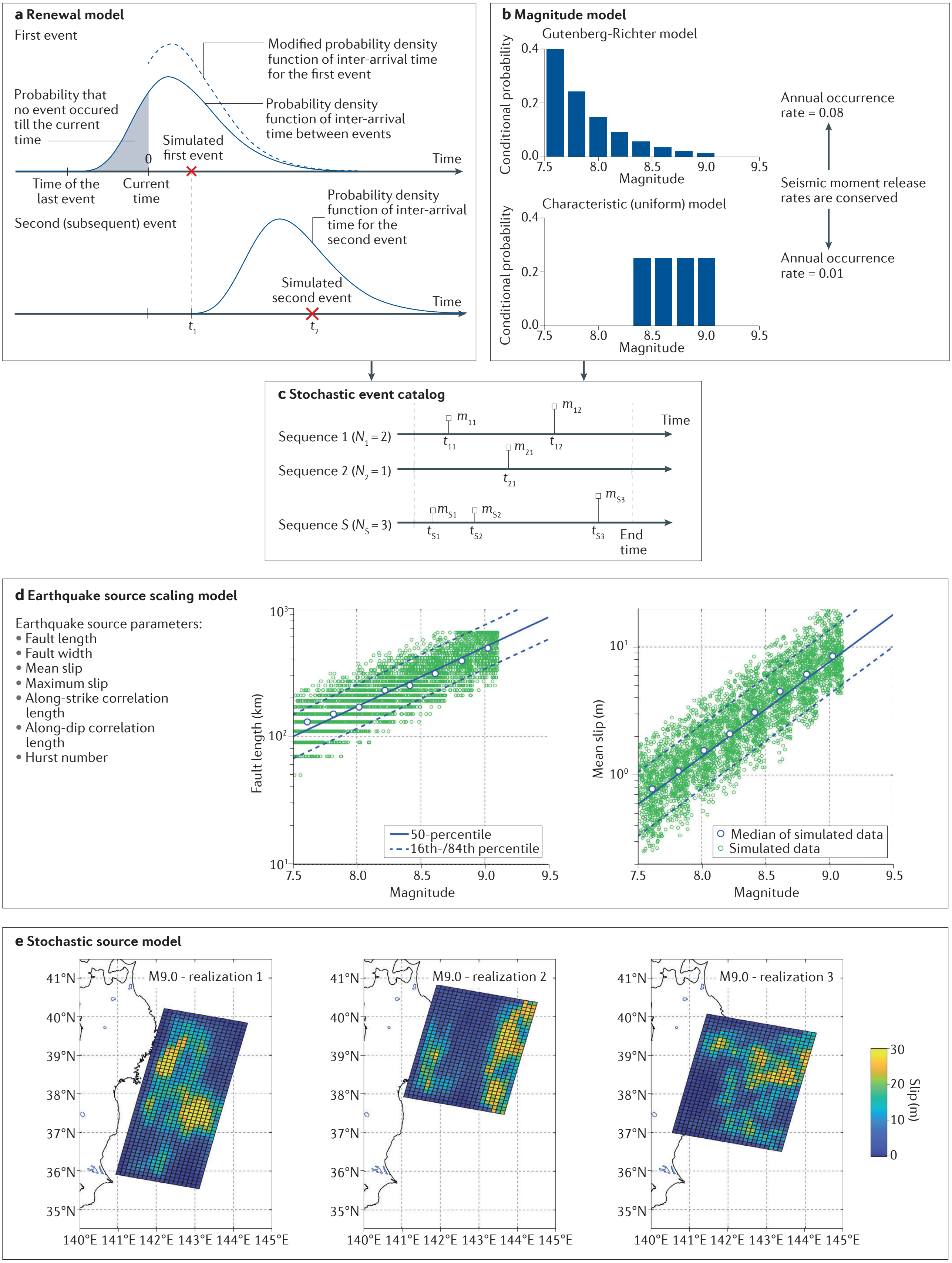

a Renewal model
First event
Modified probability density function of inter-arrival time for the first event
Probability that no event occured till the current time
Probability density function of inter-arrival time between events
Simulated first event
0
Time
Time of the last event
Current time
Second (subsequent) event
Probability density function of inter-arrival time for the second event
Simulated second event
Time
t_1
t_2
b Magnitude model
Gutenberg-Richter model
Conditional probability
Magnitude
Characteristic (uniform) model
Annual occurrence rate = 0.08
Seismic moment release rates are conserved
Annual occurrence rate = 0.01
c Stochastic event catalog
Sequence 1 (N_1 = 2)
Sequence 2 (N_2 = 1)
Sequence S (N_S = 3)
Time
End time
d Earthquake source scaling model
Earthquake source parameters:
• Fault length
• Fault width
• Mean slip
• Maximum slip
• Along-strike correlation length
• Along-dip correlation length
• Hurst number
Fault length (km)
Mean slip (m)
Magnitude
50-percentile
16th-/84th percentile
Median of simulated data
Simulated data
e Stochastic source model
M9.0 - realization 1
M9.0 - realization 2
M9.0 - realization 3
Slip (m)

Fig 5

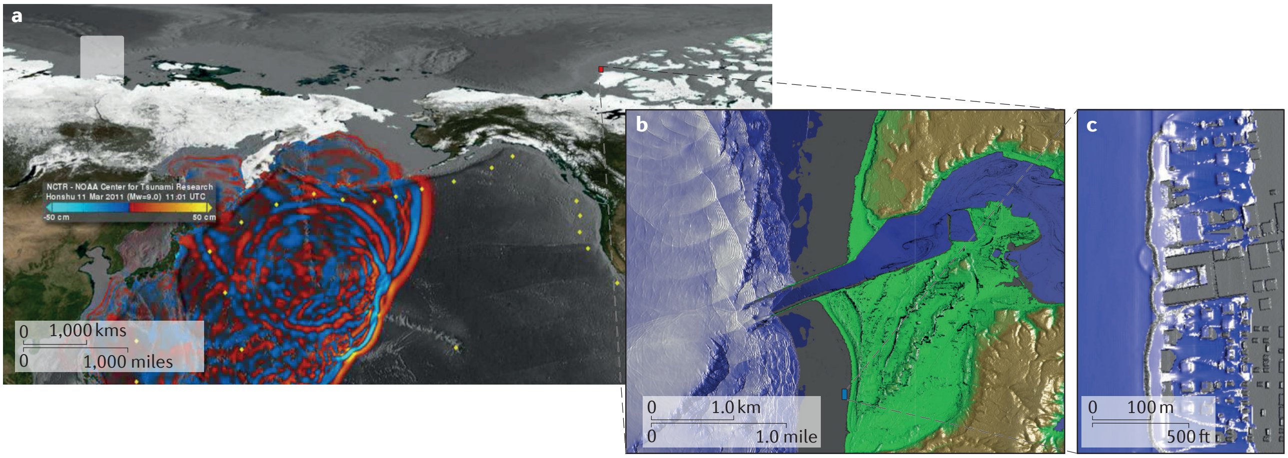
a
NCTR - NOAA Center for Tsunami Research
Honshu 11 Mar 2011 (Mw=9.0) 11:01 UTC
-50 cm
50 cm
0 1,000 kms
0 1,000 miles
b
0 1.0 km
0 1.0 mile
c
0 100 m
500 ft

Fig 6

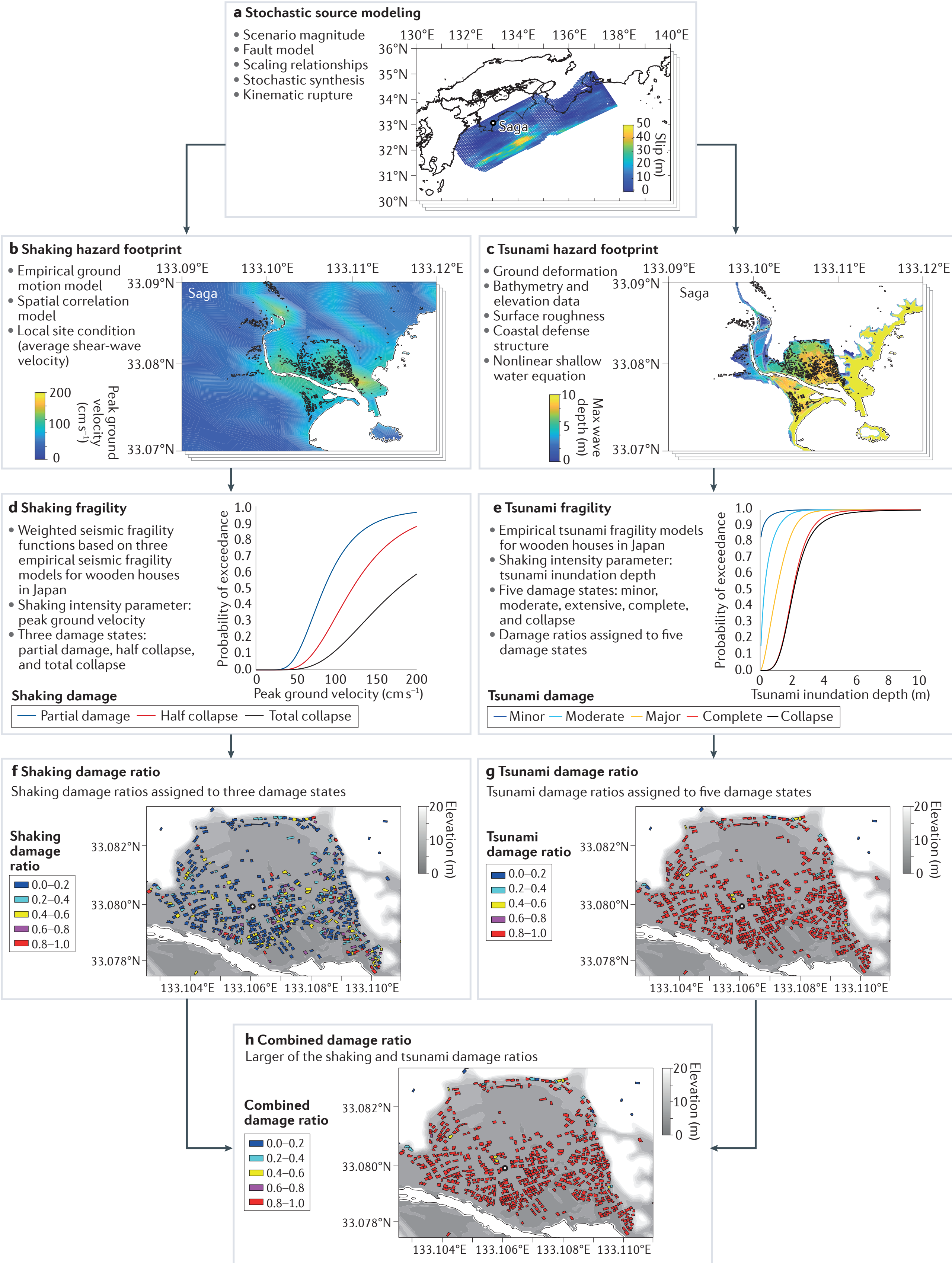

a Stochastic source modeling
• Scenario magnitude
• Fault model
• Scaling relationships
• Stochastic synthesis
• Kinematic rupture
130°E 132°E 134°E 136°E 138°E 140°E
36°N 35°N 34°N 33°N 32°N 31°N 30°N
Saga
Slip (m)
50 40 30 20 10 0
b Shaking hazard footprint
• Empirical ground motion model
• Spatial correlation model
• Local site condition (average shear-wave velocity)
133.09°E 133.10°E 133.11°E 133.12°E
33.09°N 33.08°N 33.07°N
Saga
Peak ground velocity (cm s−1)
200 100 0
c Tsunami hazard footprint
• Ground deformation
• Bathymetry and elevation data
• Surface roughness
• Coastal defense structure
• Nonlinear shallow water equation
133.09°E 133.10°E 133.11°E 133.12°E
33.09°N 33.08°N 33.07°N
Saga
Max wave depth (m)
10 5 0
d Shaking fragility
• Weighted seismic fragility functions based on three empirical seismic fragility models for wooden houses in Japan
• Shaking intensity parameter: peak ground velocity
• Three damage states: partial damage, half collapse, and total collapse
Probability of exceedance
1.0 0.9 0.8 0.7 0.6 0.5 0.4 0.3 0.2 0.1 0.0
0 50 100 150 200
Peak ground velocity (cm s−1)
Shaking damage
Partial damage
Half collapse
Total collapse
e Tsunami fragility
• Empirical tsunami fragility models for wooden houses in Japan
• Shaking intensity parameter: tsunami inundation depth
• Five damage states: minor, moderate, extensive, complete, and collapse
• Damage ratios assigned to five damage states
Probability of exceedance
1.0 0.9 0.8 0.7 0.6 0.5 0.4 0.3 0.2 0.1 0.0
0 2 4 6 8 10
Tsunami inundation depth (m)
Tsunami damage
Minor
Moderate
Major
Complete
Collapse
f Shaking damage ratio
Shaking damage ratios assigned to three damage states
Shaking damage ratio
0.0–0.2
0.2–0.4
0.4–0.6
0.6–0.8
0.8–1.0
33.082°N 33.080°N 33.078°N
133.104°E 133.106°E 133.108°E 133.110°E
Elevation (m)
20 10 0
g Tsunami damage ratio
Tsunami damage ratios assigned to five damage states
Tsunami damage ratio
0.0–0.2
0.2–0.4
0.4–0.6
0.6–0.8
0.8–1.0
33.082°N 33.080°N 33.078°N
133.104°E 133.106°E 133.108°E 133.110°E
Elevation (m)
20 10 0
h Combined damage ratio
Larger of the shaking and tsunami damage ratios
Combined damage ratio
0.0–0.2
0.2–0.4
0.4–0.6
0.6–0.8
0.8–1.0
33.082°N 33.080°N 33.078°N
133.104°E 133.106°E 133.108°E 133.110°E
Elevation (m)
20 10 0

Fig 7

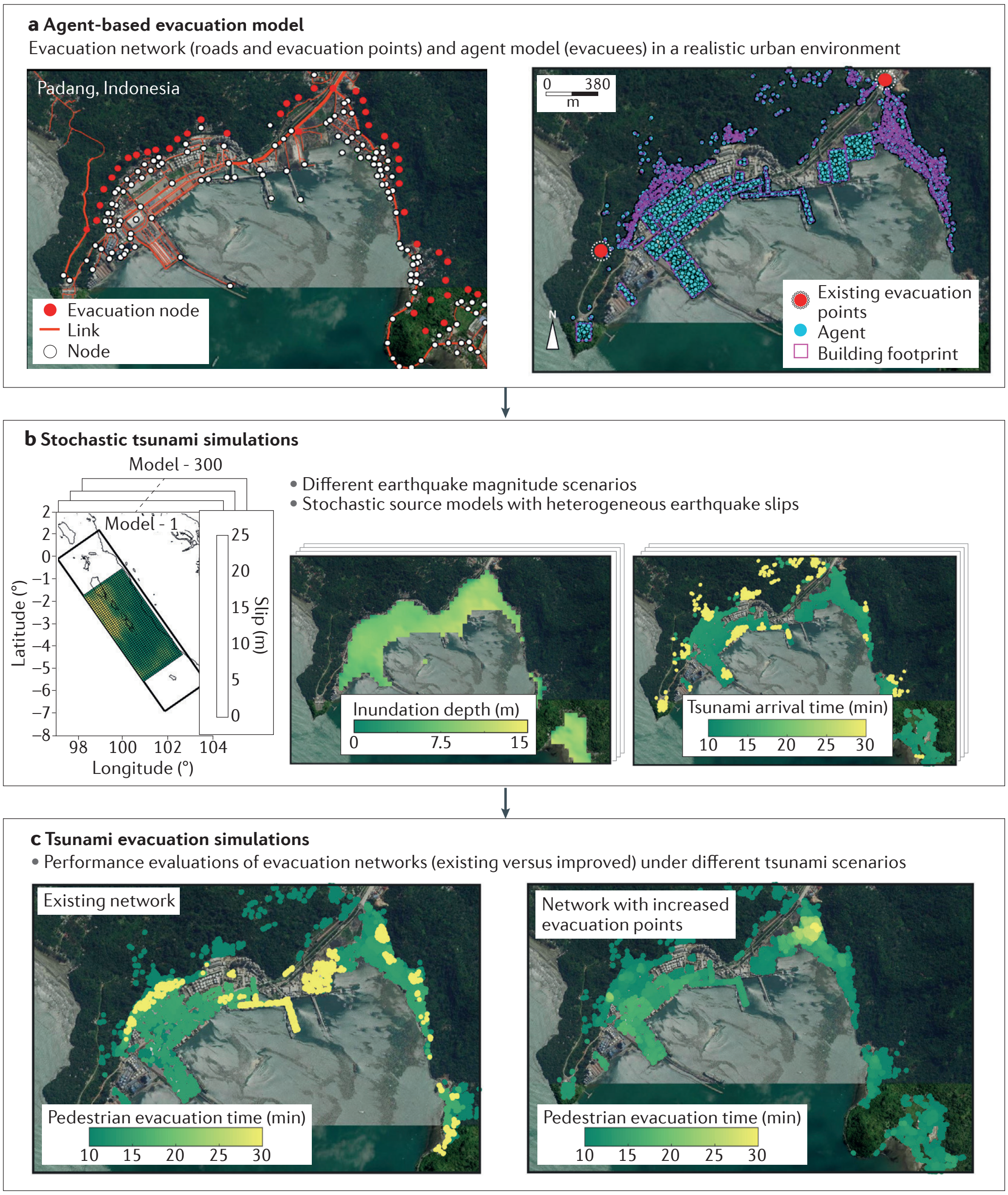

a Agent-based evacuation model
Evacuation network (roads and evacuation points) and agent model (evacuees) in a realistic urban environment
Padang, Indonesia
Evacuation node
Link
Node
0 380
m
N
Existing evacuation points
Agent
Building footprint
b Stochastic tsunami simulations
Model - 300
Model - 1
Different earthquake magnitude scenarios
Stochastic source models with heterogeneous earthquake slips
Latitude (°)
Longitude (°)
Slip (m)
25
20
15
10
5
0
98 100 102 104
Inundation depth (m)
0 7.5 15
Tsunami arrival time (min)
10 15 20 25 30
c Tsunami evacuation simulations
Performance evaluations of evacuation networks (existing versus improved) under different tsunami scenarios
Existing network
Network with increased evacuation points
Pedestrian evacuation time (min)
10 15 20 25 30